Taylor & Francis
Taylor & Francis Group

RESEARCH ARTICLE

OPEN ACCESS | Check for updates

Salivary extracellular vesicles inhibit Zika virus but not SARS-CoV-2 infection

Carina Conzelmann[a]*, Rüdiger Groß [ID][a]*, Min Zou[a,b], Franziska Krüger[a], André Görgens [ID][c,d], Manuela O Gustafsson[c], Samir El Andaloussi [ID][c], Jan Münch [ID][a,e] and Janis A. Müller[a]

[a]Institute of Molecular Virology, Ulm University Medical Center, Ulm, Germany; [b]Guangzhou Key Laboratory of Drug Research for Emerging Virus Prevention and Treatment, School of Pharmaceutical Sciences, Southern Medical University, Guangzhou, China; [c]Department of Laboratory Medicine, Karolinska Institutet, Stockholm, Sweden; [d]Institute for Transfusion Medicine, University Hospital Essen, Essen, Germany; [e]Core Facility Functional Peptidomics, Ulm University Medical Center, Ulm, Germany

ABSTRACT
Zika virus (ZIKV) is mainly transmitted via mosquitos, but human-to-human transmissions also occur. The virus is shed into various body fluids including saliva, which represents a possible source of viral transmission. Thus, we here explored whether human saliva affects ZIKV infectivity. We found that physiological concentrations of pooled saliva dose-dependently inhibit ZIKV infection of monkey and human cells by preventing viral attachment to target cells. The anti-ZIKV activity in saliva could not be abrogated by boiling, suggesting the antiviral factor is not a protein. Instead, we found that purified extracellular vesicles (EVs) from saliva inhibit ZIKV infection. Salivary EVs (saEVs) express typical EV markers such as tetraspanins CD9, CD63 and CD81 and prevent ZIKV attachment to and infection of target cells at concentrations that are naturally present in saliva. The anti-ZIKV activity of saliva is conserved but the magnitude of inhibition varies between individual donors. In contrast to ZIKV, severe acute respiratory syndrome coronavirus 2 (SARS-CoV-2), predominantly spreading via respiratory droplets, is not affected by saliva or saEVs. Our findings provide a plausible explanation for why ZIKV transmission via saliva, i.e. by deep kissing have not been recorded and establish a novel oral innate immune defence mechanism against some viral pathogens.

Introduction

Over the last 12 years, Zika virus (ZIKV) re-emerged and caused several epidemics in the Americas [1]. Infection with ZIKV remains asymptomatic, manifests as self-resolving Zika fever [2], or results in severe diseases like Guillain-Barré syndrome, a neurological disorder that can be fatal [3,4]. Devastatingly, ZIKV infection during pregnancy can induce teratogenic effects, including foetal death, microcephaly [5], and congenital complications that may impair future neurodevelopmental function [6]. Until now, no vaccine nor drugs are available, thus ZIKV poses a risk especially for pregnant women. ZIKV is mainly spread via the *Aedes aegypti* and *albopictus* mosquitos and transmissions have been recorded in 87 countries and territories [7] and still occur in different regions [8,9]. Independent of mosquitos, ZIKV can be transmitted via body fluids [10]. In infected individuals, the virus has been detected in plasma, cerebrospinal fluid, amniotic fluid, urine,

semen, vaginal excretions, breast milk, and saliva [10,11]. Transmissions via some of these body fluids, i.e. during blood transfusion [10,12], intrauterine [10,13], sexual intercourse [10,14–16] or breastfeeding [17] have been recorded. Even though there is no evidence at present that ZIKV can be transmitted through saliva, i.e. during deep kissing [18–20], this route of transmission cannot be excluded as there have been cases of unresolved human-to-human non-sexual transmissions [21,22]. ZIKV RNA is regularly detected in saliva [10,11,23–28] which might be relevant for diagnostic purposes as RNA levels are as high as up to $\sim 10^6$ per ml [24] and remain detectable up to 91 days [25]. Importantly, infectious virus has been isolated from saliva [24,28] suggesting that this body fluid represents a potential source of viral transmission. Animal studies confirmed that ZIKV is present in saliva and suggested that rhesus macaque saliva may contain anti-ZIKV activity [29]. In addition, rhesus macaques that were repeatedly

challenged with saliva from ZIKV-positive animals remained uninfected [29], suggesting a low risk of oral mucosal transmission. As human saliva was previously reported to contain antimicrobial and antiviral activity [30] we here analysed the effect of human saliva on ZIKV infection. We found that saliva inhibits ZIKV infection by preventing ZIKV attachment to target cells. The responsible factors are extracellular vesicles (EVs) that are highly abundant in saliva and compete with ZIKV for cellular interaction, representing a novel antiviral defence mechanism. Intriguingly, we found that the currently pandemic SARS-CoV-2 is not inhibited by either saliva or purified salivary EVs, matching its dominant mode of transmission by saliva-containing respiratory droplets.

Materials and methods

Cell culture

Vero E6 (*Cercopithecus aethiops* derived epithelial kidney) cells were grown in Dulbecco's modified Eagle's medium (DMEM) which was supplemented with 2.5% heat-inactivated foetal calf serum (FCS), 100 units/ml penicillin, 100 μg/ml streptomycin, 2 mM L-glutamine, 1 mM sodium pyruvate, and non-essential amino acids (Sigma #M7145). Adenocarcinomic basal epithelial cells (A549), carcinomic cervical epithelial cells (HeLa), Caco-2 (human epithelial colorectal adenocarcinoma) cells, and primary human foreskin fibroblasts (HFF; kindly provided by the Institute of Virology, Ulm) were grown in DMEM which was supplemented with 10% heat-inactivated FCS, 100 units/ml penicillin, 100 μg/ml streptomycin and 2 mM L-glutamine. Primary gingival fibroblasts (ATCC PCS-201-018) were grown in fibroblast basal medium (ATCC PCS-201-030) supplemented with fibroblast growth kit-low serum (ATCC PCS-201-041). For experiments in the presence of saliva, the medium was supplemented with 100 μg/ml gentamicin. All cells were grown at 37°C in a 5% CO_2 humidified incubator.

Virus strains and virus propagation

The African ZIKV strain MR766 was isolated in 1947 from a sentinel rhesus macaque [31]. Asian and pathogenic strains PRVABC59 or FB-GWUH-2016 were isolated in 2015 from a human serum specimen [32] or from a foetal brain with severe abnormalities [13], respectively. In brief, 70% confluent Vero E6 cells in 175 cm^2 cell culture flasks were inoculated with ZIKV in 5 ml medium for 2 h, before 40 ml medium was added. Cells were monitored for 3 to 5 days and supernatant was harvested when 70% of the cells detached due to cytopathic effects. SARS-CoV-2 isolates BetaCoV/France/IDF0372/2020 (#014 V-03890) and BetaCoV/Netherlands/01/NL/2020 (#010 V-03903) were obtained through the European Virus Archive global. Virus was propagated by inoculation of 70% confluent Vero E6 in 75 cm^2 cell culture flasks with 100 μl SARS-CoV-2 isolates in 3.5 ml serum-free medium containing 1 μg/ml trypsin. Cells were incubated for 2 h at 37°C, before adding 20 ml medium containing 15 mM HEPES. Cells were incubated at 37°C and supernatant harvested at day 3 post-inoculation when a strong cytopathic effect (CPE) was visible. Supernatants were centrifuged for 3 min at 325 × g to remove cellular debris, and then aliquoted and stored at −80°C as virus stocks. Infectious virus titre was determined by endpoint titration.

$TCID_{50}$ endpoint titration

To determine the tissue culture infectious dose 50 ($TCID_{50}$), virus stocks were serially diluted 10-fold and used to inoculate Vero E6 cells. To this end, 6,000 Vero E6 cells were seeded per well in 96 flat bottom well plates in 100 μl medium and incubated overnight before 80 μl fresh medium was added. Next, 20 μl of titrated virus of each dilution was used for inoculation, resulting in final virus dilutions of $1:10^1$ to $1:10^9$ on the cells in triplicates. Cells were then incubated for at least 6 days and monitored for CPE. $TCID_{50}$/ml was calculated according to Reed and Muench.

Quantitative real-time PCR (qRT-PCR)

Viral genome copy numbers were assessed by qRT-PCR. For this, viral RNA lysates were prepared by mixing supernatants 1:1 with direct lysis buffer containing 10 mM Tris-HCl pH 7.4, 0.5% IGEPAL CA-630 (Alfa Aesar), 100 mM NaCl and 10 μl/ml RNAsin Plus (Promega) and incubating at room temperature for 5 min [33]. 5 μl of this were then used as RNA template in a 20 μl qRT-PCR reaction containing 1X TaqMan Fast 1 Step Virus Master Mix, RKI-F and -R (8 pmol final concentration each) and RKI-S (3 pmol final concentration) and DEPC-treated water up to 20 μl. The reaction was then run on a StepOnePlus qRT-PCR cycler (ABI) as follows: 1) 50°C, 5 min (reverse transcription), 2) 95°C, 20 s (reverse transcriptase inactivation & initial denaturation), 3) 95°C, 3 s – 60°C, 30 s (amplification, 50x repeated). Synthetic ZIKV RNA (ATCC VR-3252SD) served as a standard and Ct values

were fit to the known concentrations to enable quantification of the unknowns.

Primer sequences:

ZIKV-RKI-F (ACGGCYCTYGCTGGAGC)

ZIKV-RKI-R (GGAATATGACACRCCCTTCAAYCTAAG)

ZIKV-RKI-S (FAM-AGGCTGAGATGGATGGTGCAAAGGG-BNQ535)

Saliva

Human saliva was obtained from healthy volunteers at Ulm University. Individual samples were collected into 50 ml Falcon tubes immediately before they were centrifuged 3,000 × g for 5 min to remove cell debris. The supernatant was either directly used for further analysis (fresh saliva) or after storage at −80°C. For testing of pooled saliva, equal volumes of individual donors were mixed after centrifugation. All procedures were approved by the local ethics committee of Ulm University (89/17).

Cell viability assays

The effect of saliva on the metabolic activity of the cells was analysed using the CellTiter-Glo® Luminescent Cell Viability Assay (Promega #G7571) or based on the reduction of the tetrazolium dye MTT (3-(4,5-dimethylthiazol-2-yl)-2,5-diphenyltetrazolium bromide). Metabolic activity was examined under conditions corresponding to the respective infection assays. The CellTiter-Glo® assay was performed according to the manufacturer's instructions. Briefly, medium was removed from the culture after 2 days of incubation and 50% substrate reagent in PBS was added. After 10 min, luminescence of the samples was measured in an Orion II Microplate Luminometer (Titertek Berthold). For the MTT assay, after medium removal, 100 μl of 1:10 PBS-diluted MTT stock solution (5 mg/ml in PBS; Sigma Aldrich) was added. After 2.5 h of incubation, the supernatant was discarded and formazan crystals were dissolved in 100 μl 1:1 DMSO-ethanol. Absorption was measured at 450 nm and baseline was corrected at 650 nm using a Vmax kinetic microplate reader (Molecular Devices). Untreated controls were set to 100% viability.

Infection and cell-based ZIKV immunodetection assay

To determine ZIKV infection, 6,000 target cells per well were seeded in 96 well plates in 100 μl medium, incubated overnight, and inoculated with the saliva samples and the desired multiplicity of infection (MOI) of ZIKV in a total volume of 200 μl. After 2 hours the medium was replaced by fresh medium and 2 days later infection quantified by detecting flavivirus E protein as described [34]. To this end, the medium was discarded and the cells washed with PBS before fixation with 4% paraformaldehyde in PBS (PFA) for 20 min at room temperature. After aspirating PFA, cells were permeabilized for 5 min by incubation with 100% ice cold methanol, and again washed with PBS. Then, cells were incubated with 1:10,000 diluted mouse anti-flavivirus protein E antibody 4G2 (Absolute Antibody #Ab00230-2.0) in antibody buffer (PBS containing 10% (v/v) FCS and 0.3% (v/v) Tween 20) at 37°C. After 1 hour, the cells were washed three times with washing buffer (0.3% (v/v) Tween 20 in PBS) before a secondary anti-mouse antibody conjugated with HRP (Thermo Fisher #A16066) was added and incubated for 1 h at 37°C. Following four times of washing, TMB peroxidase substrate (Medac #52-00-04) was added. After 5 min light-protected incubation at room temperature the reaction was stopped using 0.5 M H_2SO_4. The optical density (OD) was recorded at 450 nm and baseline corrected for 650 nm using the VMax Kinetic ELISA microplate reader (Molecular Devices). Values were corrected for the background signal derived from uninfected cells and untreated controls were set to 100% infection.

Fluorescence microscopy

For fluorescence microscopy, fixation and permeabilization were performed as aforementioned. Cells were then stained with 1:1,000 diluted mouse anti-flavivirus protein E antibody 4G2 and 1:400 diluted goat anti-mouse secondary antibody conjugated to Alexa Fluor 647 (ThermoFisher Scientific #A21235). After washing, nuclei were stained with 1:2,000 diluted Hoechst 33342 (10 μg/ml stock in H_2O, ThermoFisher Scientific, H1399), incubated for 10 min at room temperature. Imaging was then performed in a Cytation 3 Microplate Reader/Microscope using Gen5 software (Biotek).

ZIKV virion attachment assay

150,000 Vero E6 cells were seeded in eight-well μ-Slides (Ibidi #80,826) and incubated overnight. In a total volume of 300 μl, cells were inoculated with ZIKV MR766 (MOI 35) in the presence of saliva samples and incubated for 2 h at 4°C. Subsequently, the inoculum was removed and cells were fixed with 4% PFA for 10 min at 4°C. Afterwards, cells were washed

with PBS. Unspecific binding sites were blocked by 30 min incubation with 5% (v/v) FCS and 1% (v/v) bovine serum albumin (BSA) in PBS. Viruses were stained with 1:10,000 diluted mouse anti-flavivirus protein E antibody 4G2 (Absolute Antibody #Ab00230-2.0) in PBS with 1% (v/v) BSA for 45 min. After three washing steps with PBS, samples were incubated with 1:1,000 diluted goat anti-mouse secondary antibody conjugated to Alexa Fluor 647 (ThermoFisher Scientific #A21235) for 45 min. Cell nuclei were stained with 1:2,000 diluted Hoechst 33342 (ThermoFisher Scientific #H1399) for 20 min. Attached virus particles were imaged as z-stacks of 25 slices of 0.55 μm by confocal microscopy using a Zeiss LSM 710. Images were processed and combined to maximum intensity projections using the ZEN 2.3 (blue edition) software. Attached ZIKV virions were quantified using a custom ImageJ (Fiji) macro, that automatically identifies and counts local fluorescence maxima of a set of 1024×1024 px confocal images (noise tolerance: 50,000).

SARS-CoV-2 infection and inhibition assay

To determine SARS-CoV-2 infection, 30,000 Caco-2 target cells were seeded in 96 well plates in 100 μl. The next day, fresh medium was added, saliva was mixed with virus or saEVs were added and the cells inoculated with SARS-CoV-2 in a total volume of 180 μl. Two days later, infection was quantified by detecting SARS-CoV-2 S protein. To this end, cells were fixed by adding 180 μl 8% PFA and 30 min of room temperature incubation. Medium was then discarded and cells permeabilized for 5 min at room temperature by adding 100 μl of 0.1% Triton in PBS. Cells were washed with PBS and stained with 1:5,000 diluted mouse anti-SARS-CoV-2 S protein antibody 1A9 (Biozol GTX-GTX632604) in antibody buffer (PBS containing 10% (v/v) FCS and 0.3% (v/v) Tween 20) at 37°C. After 1 hour, the cells were washed three times with washing buffer (0.3% (v/v) Tween 20 in PBS) before a secondary anti-mouse antibody conjugated with HRP (Thermo Fisher #A16066) was added (1:15,000) and incubated for 1 h at 37°C. Following four times of washing, the TMB peroxidase substrate (Medac #52-00-04) was added. After 5 min light-protected incubation at room temperature, the reaction was stopped using 0.5 M H_2SO_4. The optical density (OD) was recorded at 450 nm and baseline corrected for 620 nm using the Asys Expert 96 UV microplate reader (Biochrom). Values were corrected for the background signal derived from uninfected cells and untreated controls were set to 100% infection.

Preparation of extracellular vesicles (EVs)

A filtration-ultrafiltration protocol (F-UF) was applied to prepare EVs from pooled urine, saliva or individual saliva donors. For this purpose, fresh saliva was centrifuged for 5 min at $3,000 \times g$ to pellet cellular debris and the supernatant collected (separately or pooled). Saliva was then threefold diluted with PBS (Gibco) and 0.45 μm syringe-filtered (for individual donors) or vacuum filtered (for pooled saliva). Filtered saliva was then loaded onto 100 kDa ultrafiltration devices (Amicon Ultra-15 100 kDa MWCO filters (Millipore, Sigma Aldrich #Z740208) or Sartorius Vivaspin 20 100 kDa (Sigma Aldrich, #Z614661)) and centrifuged at $3,220 \times g$ for 60 min. For urine, the same protocol without dilution by PBS was applied. The throughflow was discarded and centrifugation was repeated until the entire volume was concentrated. The EV-containing retentate was immediately used or stored at −80°C.

To purify EVs from residual soluble proteins and impurities we applied an optimized protocol combining tangential flow filtration (TFF) with subsequent bind-elute size exclusion chromatography (BE-SEC) which we have described previously [35]. Briefly, saliva or vaginal lavage from 10 or seminal plasma from 50 donors was subjected to low-speed centrifugation at $700 \times g$ for 5 minutes, followed by $2,000 \times g$ spin for 10 minutes to remove larger particles and cell debris. The supernatant was then pooled, diluted fourfold in sterile PBS (Gibco, pH 7.4) and filtered through an 0.22 μm syringe filter (VWR, cellulose acetate membranes). The filtrate was diafiltrated with two volumes of sterile PBS and concentrated to 20 ml using a KR2i tangential flow filtration system (SpectrumLabs) with 300 kDa cut-off hollow fibres at a flow rate of 100 ml/min (transmembrane pressure at 3.0 psi and shear rate at $3,700 \text{ s}^{-1}$). The pre-concentrated sample was subsequently loaded onto BE-SEC columns (HiScreen Capto Core 700 column, GE Healthcare Life Sciences), connected to an ÄKTAstart chromatography system (GEHealthcare Life Sciences). Flow rate settings for column equilibration, sample loading and column cleaning in place (CIP) procedure were chosen according to the manufacturer's instructions. The EV sample was collected according to the 280 nm UV absorbance chromatogram and concentrated using an Amicon Ultra-15 10 kDa molecular weight cut-off spin-filter (Millipore) and stored as aliquots at −80°C for further downstream analysis.

Multiplex bead-based EV surface protein profiling by flow cytometry

Purified EVs were subjected to bead-based multiplex EV analysis (MACSPlex Exosome Kit, human,

Miltenyi Biotec) as previously described [36,37]. Briefly, EVs purified by TFF/BE-SEC were diluted at input doses of 1×10^9 NTA-quantified particles per assay in a total of 60 μl MACSplex buffer and incubated overnight with 3 μl MACSPlex Exosome Capture Beads on an orbital shaker at 450 rpm at room temperature. Beads were washed with 200 μl MACSPlex buffer and the liquid was removed by applying vacuum (Sigma-Aldrich, Supelco PlatePrep; −100 mBar) to the MACSPlex 96 well 0.22 μm filter plate. For counter staining of captured EVs, a mixture of individual APC-conjugated anti-CD9, anti-CD63 or anti-CD81 detection antibodies or a mixture of all three antibodies (supplied in the MACSPlex kit, 4 μl each) were added to each well in a total volume of 135 μl and the plate was incubated at 450 rpm for 1 h at room temperature in the dark. Next, the samples were washed twice in PBS and liquid removed twice before resuspension in 150 μl MACSPlex buffer. Samples were then transferred to a V-bottom 96-well microtiter plate (Thermo Scientific) and analysed by flow cytometry using a MACSQuant Analyzer 10 flow cytometer (Miltenyi Biotec). FlowJo software (version 10.5.3, FlowJo, LLC) was used to analyse flow cytometric data. Median fluorescence intensities (MFI) for all 39 capture bead subsets were background-corrected by subtracting respective MFI values from matched non-EV containing buffer controls that were treated exactly like EV samples (buffer + capture beads + antibodies). Unless mentioned otherwise all steps were performed as described before [37].

Liposome preparation

Liposomes were prepared by thin-film hydration and extrusion. DOPC (1,2-dioleoyl-sn-glycero-3-phosphocholine, Avanti Polar Lipids) was added to a glass round-bottom flask. The solvent was then evaporated by slowly applying a vacuum at a Schlenk line. The vacuum was held for 2 h and then purged with argon. Next, the lipid film was hydrated by adding PBS, yielding a total lipid concentration of 50 mM. The flasks were shaken at 37°C, 180 rpm, for 1 h. Small unilamellar vesicles were then prepared by 100x extrusion through 0.2 μM polycarbonate membranes (Nuclepore Track-Etched Membrane, Whatman) in a Mini Extruder (Avanti Polar Lipids) and liposomes finally quantified by nanoparticle tracking analysis (NTA) using a ZetaView (ParticleMetrix) as described below.

Saliva and saEV treatments

Denaturation: Saliva and saEV samples were boiled at 99°C for 20 min in an Eppendorf Thermomixer. Samples were then centrifuged for 15 min at 20,000 × g. The pellets were then discarded and the supernatants used for further analysis. Proteinase K digestion: SaEVs were incubated with 300 μg/ml proteinase K (Roche #03115887001) for 2 h at 37°C. To stop proteinase K activity, the sample was denatured and centrifuged as described above and the supernatants used for further analysis. Benzonase ® nuclease digestion: $MgCl_2$ was added at a final concentration of 1 mM to saEVs to ensure activity of Benzonase ®. Digestion was then carried out with 25 Units Benzonase ® nuclease (Sigma Aldrich, #E1014-25KU) for 2 h at room temperature. EV depletion by ultrafiltration: Pooled and centrifuged saliva (3,000 x g, 5 min) was loaded onto 100 kDa ultrafiltration devices (as for F-UF, see above) and centrifuged at 3,220 x g for 1 h. The flowthrough was collected and the retentate resuspended in PBS to yield the original volume.

Nanoparticle tracking analysis

Nanoparticle tracking analysis (NTA) to determine the concentration and the size distribution of particles in saliva and EV isolations was performed using a ZetaView TWIN (Particle Metrix). To this end, the samples were diluted in particle-free PBS and videos of the light-refracting particles were recorded with the following settings: 25°C fixed temperature, 11 positions, 1 cycle, sensitivity 85, shutter 100, 15 fps, 2 s videos/position, 3–5 measurements. The number and size distribution were evaluated by ZetaView Analyze 08.05.05 SP2. Between the samples, the chamber was thoroughly flushed with particle-free PBS.

Determination of protein concentration

The protein content of samples was quantified using Pierce™ Rapid Gold BCA Protein Assay Kit as described by the manufacturer (Thermo Fisher #A53225) using the microwell procedure.

SDS-PAGE and Western Blot

To confirm protein denaturation, saliva and saEV samples were mixed with Protein Loading Buffer (LI-COR #928-40004) and TCEP (50 mM final concentration) and heated to 70°C for 10 min. Proteins were then separated on NuPAGE 4–12% BisTris gels, fixed with a 50% methanol: 7% acetic acid solution and stained with GelCode Blue

(Thermo Fisher #24590) for 1 h at room temperature. After destaining with ultrapure water, the gel was imaged on a LI-COR Odyssey near-infrared imager.

To determine levels of EV- and saliva-specific markers in EV isolations, protein content was first determined by BCA assay as described. Concentrations were then adjusted to that of the lowest-concentrated sample with PBS. Concentration-adjusted samples were mixed with Protein Loading Buffer (LI-COR #928-40004) and TCEP (Sigma Aldrich, 50 mM final concentration) and heated to 70°C for 10 min. Proteins were then separated on NuPAGE 4–12% BisTris gels, blotted onto Immobilon-FL PVDF membranes via semi-dry transfer and blocked with 0.5% Casein in PBS (Thermo Scientific #37528). Membranes were then stained with primary antibodies (in 0.05% casein PBS + 0.2% Tween 20) against CD9 (Cell Signaling #CS-13174), salivary α-amylase (Abcam #ab119493), lysozyme (Novus Biologicals #NBP2-61118), flotillin-1 (Cell Signaling #CS-18634) and Alix (Cell Signaling, #CS2171) and detected with Infrared Dye labelled secondary antibodies (LI-COR IRDye). Signals were detected using a LI-COR Odyssey.

Transmission electron microscopy

Samples were adsorbed on glow discharged carbon-coated copper grids (Electric glow discharger Edwards High Vacuum) for 1 min at room temperature. Next, the grids were washed 3 times for 3 s in distilled H_2O and negatively stained with 2% (w/v) uranyl acetate in H_2O by another three incubation periods of 3 s. Excess solution was removed by filter paper and samples were allowed to dry. Samples were imaged with a JEOL JEM1400 transmission electron microscope at an accelerating voltage of 115 kV.

Statistical analysis

Determination of the inhibitory concentration 50 (IC_{50}) by the nonlinear regression [Inhibitor] vs. normalized response, correlation analyses (Pearson correlation coefficients, two-tailed p-value), and one-way ANOVA followed by Bonferroni's multiple comparison test were performed using GraphPad Prism version 8.1.0 for Windows, GraphPad Software, San Diego, California USA, www.graphpad.com.

Results

Saliva inhibits infection by different ZIKV strains in simian and human cells

To determine the effect of saliva on ZIKV infection, Vero E6 cells were inoculated with the African ZIKV MR766 strain [31] in the presence of up to 20% of pooled, cell-free human saliva. We applied a multiplicity of infection (MOI) of 0.3 which corresponds to 1.03×10^5 ZIKV RNA copies per ml and reflects the maximally detectable ZIKV concentrations in saliva [26,28]. Infection rates were determined 2 days later by a ZIKV-E protein-specific in-cell immunodetection assay [34]. As shown in Figure 1(a), saliva reduced ZIKV infection in a dose-
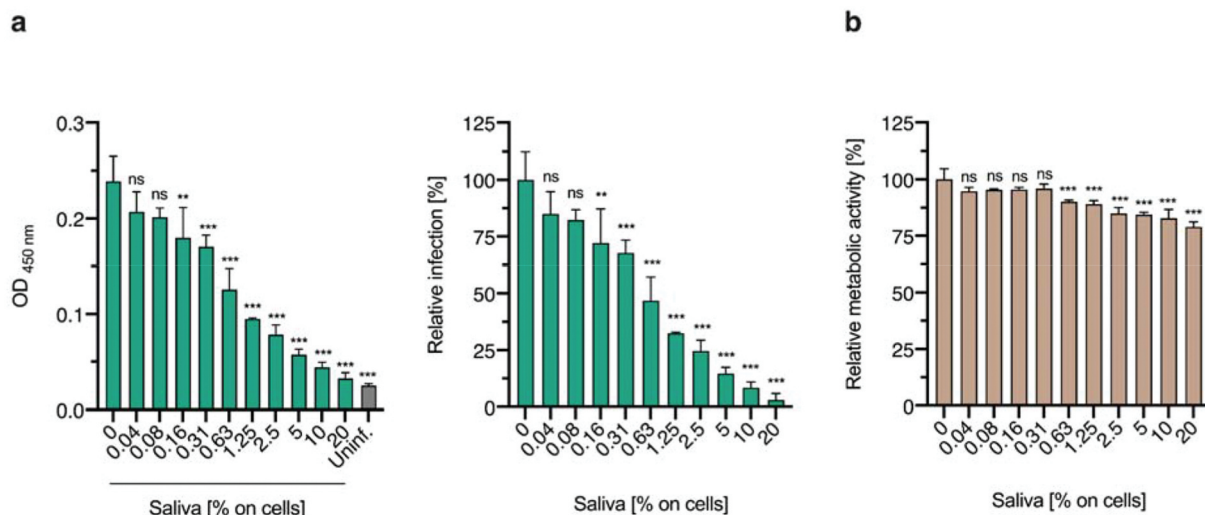
Figure 1. Saliva inhibits ZIKV MR766 infection of Vero E6 cells. (a) Saliva pooled from ten donors was serially diluted, mixed 2:1 with ZIKV MR766 and incubated for 30 min at room temperature. The mixture was added to Vero E6 cells (MOI 0.3) resulting in the final indicated cell culture concentrations. 2 hours later medium was changed and 2 days later infection was quantified by immunodetection assay that enzymatically quantifies the flavivirus protein E. Measured raw data (left) were normalized to infection rates in the absence of the respective saliva sample (right). Data are represented as average values obtained from triplicate infections ± standard deviations. (b) Vero E6 cells were incubated with pooled saliva at indicated concentrations for 2 hours. Medium was then replaced and the cellular viability determined 2 days later by CellTiter-Glo® Luminescent Cell Viability Assay. Data are normalized to viability in the absence of saliva. ns not significant; **P < 0.01; ***P < 0.001 (by one-way ANOVA with Bonferroni post-test).

dependent manner with a half-maximal inhibitory concentration (IC_{50}) of only 0.56% (v/v). Almost complete inhibition of viral infection was observed in the presence of 20% of saliva (Figure 1(a)). At this concentration, pooled saliva did not have substantial effects on cell viability (Figure 1(c)), suggesting the presence of factors with specific anti-ZIKV activity.

Saliva also blocked infection by recent Asian/American ZIKV strains that were derived from an infected foetal brain (FB-GWUH-2016) [13] or a human serum specimen (PRVABC59) [32] (Figure 2(a)). Again, both strains were inhibited with IC_{50} values of 1.01% for PRV and 1.80% for GWUH (Figure 2(a)). As Vero E6 cells are of simian origin, we next tested whether saliva may also block ZIKV infection of human cells. As shown by in-cell immunodetection

assay (Figure 2(b)) and fluorescence microscopy (Figure 2(c)), saliva suppressed ZIKV MR766 infection of primary foreskin fibroblasts (HFF), adenocarcinomic basal epithelial cells (A549), and carcinomic cervical epithelial cells (HeLa) with comparable activity. Thus, saliva has broad anti-ZIKV activity in monkey and human cells.

Saliva blocks ZIKV attachment to the cell

In order to study whether the antiviral factor in saliva targets the virion or the cell, ZIKV particles were mixed with up to 90% of saliva, and these mixtures were then used to inoculate Vero E6 cells, resulting in a 10-fold dilution and final cell culture concentrations of up to 9% (virus treatment). Simultaneously, saliva was added directly to
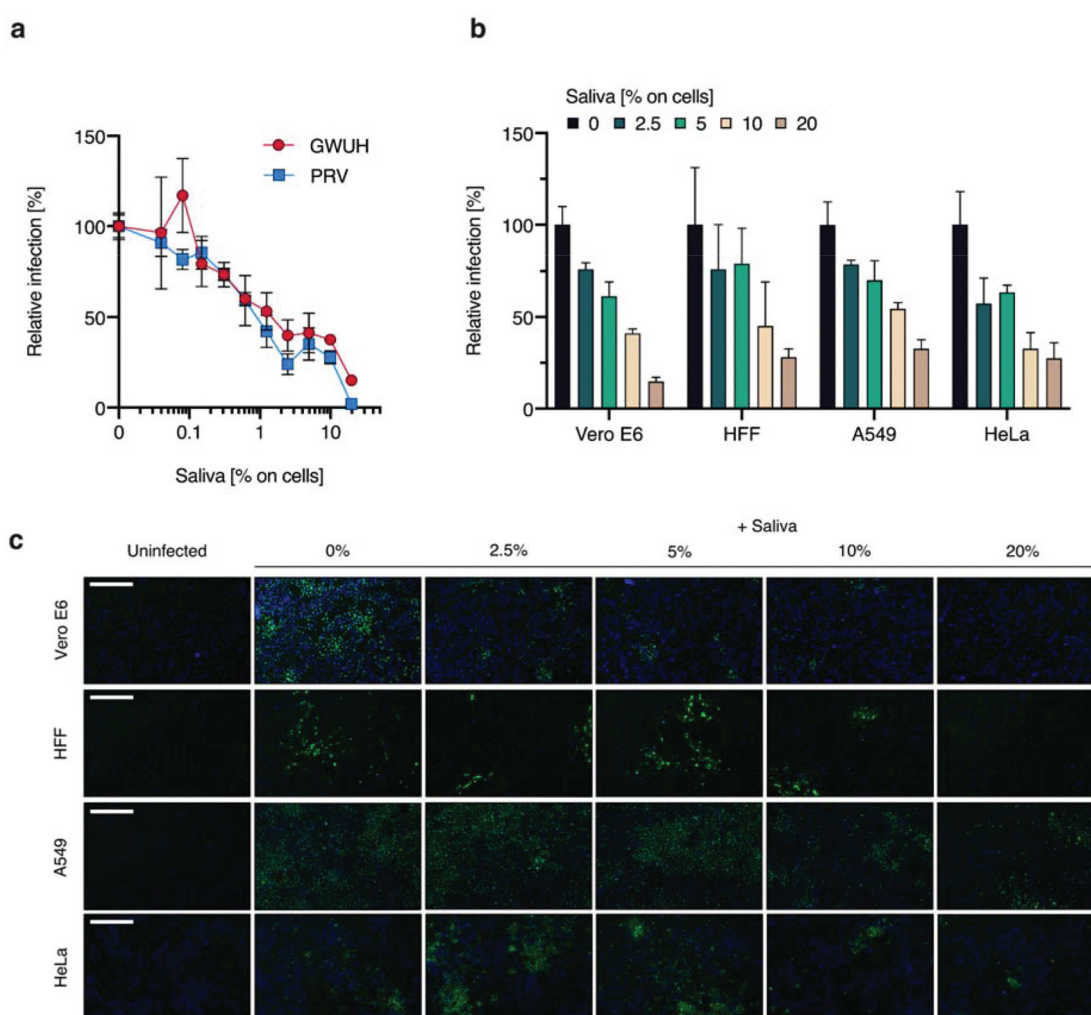
Figure 2. Saliva has broad anti-ZIKV activity. (a) Saliva pooled from ten donors was serially diluted, mixed 2:1 with ZIKV GWUH or PRV and incubated for 30 min at room temperature. The mixtures were then added to Vero E6 cells (MOI 0.6) resulting in the indicated concentrations. 2 hours later medium was changed and 2 days later infection was quantified by immunodetection assay that enzymatically quantifies the flavivirus protein E. (b and c) Pooled saliva was mixed with ZIKV MR766 and incubated for 30 min at room temperature. The mixture was added to Vero E6, HFF, A548 and HeLa cells resulting in the indicated concentrations and medium was changed 2 hours after inoculation. 2 days later infection was determined by b) immunodetection assay or c) immunofluorescent staining and fluorescence microscopy; scale bar: 500 µM. Data in a) and b) are normalized to infection rates in the absence of the respective sample and represented as average values obtained from triplicate infections ± standard deviations.

cells at concentrations of up to 9% of the body fluid, and cells were subsequently infected (cell treatment). Infection rates were determined by in-cell immunodetection assay two days later, and showed that i) high saliva concentrations during virion treatment did not result in a more potent inhibition of infection, and that ii) the saliva concentration during cell treatment determines the magnitude of the antiviral effect (Figure 3(a)). Thus, the inhibitory activity in saliva does not directly inactivate or neutralize ZIKV infectivity. Therefore, we next analysed whether saliva may block ZIKV attachment to the cell. To this end, we visualized ZIKV particle attachment by confocal microscopy. Cells were exposed to a high MOI of ZIKV particles in the absence or presence of saliva for 2 hours at 4°C. Thereafter, cells were washed, virions stained with a fluorescent antibody against the viral E protein and imaged (Fig. S1). As shown in a quantitative manner in Figure 3(b), the number of ZIKV particles that attached to the cells decreased substantially in the presence of saliva. However, the saliva concentrations required for half-maximal inhibition of viral infection were approximately 30-fold higher as those obtained in experiments where a lower MOI was used (compare with Figures 1(a) and (2a)). To directly assess whether the antiviral activity of saliva is affected by the viral dose, cells were exposed to saliva concentrations of up to 10% and subsequently infected with increasing amounts of virus. No antiviral activity of saliva was observed upon infection with the highest MOI of 36.5 (Figure 3(c)) which corresponds to 1.26×10^7 ZIKV RNA copies per ml, a number that exceeds one log of what has been maximally detected in saliva [24].

However, when lower and more physiological virus concentrations (MOI: 9.1–0.14 corresponding to 3.14×10^6–4.82×10^4 RNA copies per ml) were used, saliva inhibited ZIKV infection in a dose-dependent manner (Figure 3(c)). Collectively, these data suggest that the antiviral activity in saliva competitively blocks ZIKV attachment to target cells.

The anti-ZIKV activity of saliva is temperature resistant

If a salivary protein or polypeptide is responsible for the anti-ZIKV activity, heat treatment of saliva should denature it and abrogate viral inhibition. This was not the case, as saliva that was incubated at 90°C for 1 hour had similar antiviral activity as samples incubated at 37°C, 22°C, and 4°C (Figure 4(a)). Even pooled saliva that was boiled for 20 minutes and centrifuged to deplete the denatured proteins retained its anti-ZIKV activity (Figure 4(b)). Moreover, saliva that was stored for 3 hours at −20°C or −80°C remained antivirally active (Figure 4(c)). These results show that proteins are likely not involved in the anti-ZIKV activity of saliva and that pooled saliva can be frozen without a loss in activity.

Extracellular vesicles prepared from saliva inhibit ZIKV infection

We previously found that semen inhibits ZIKV infection and that highly abundant extracellular vesicles (EVs) in semen are responsible for this effect [38]. Similar to the results described above for saliva,
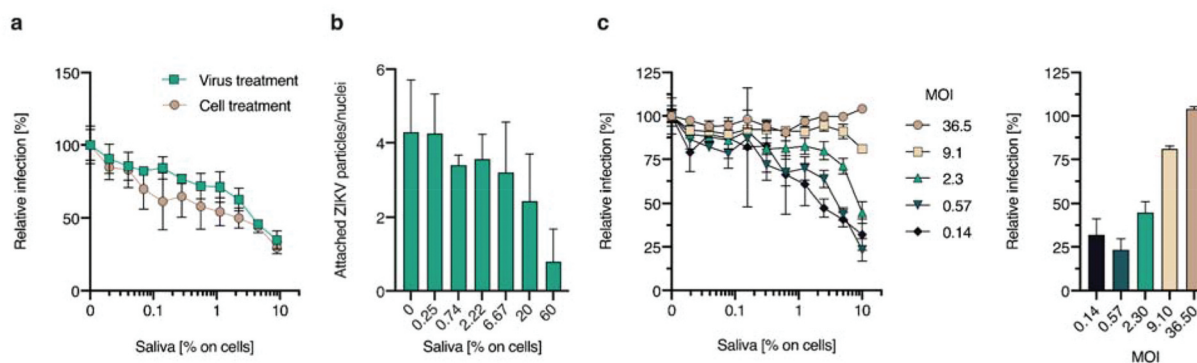

Figure 3. Saliva inhibits ZIKV attachment. (a) For virus treatment ZIKV MR766 was mixed with pooled saliva (concentrations: 0.18, 0.35, 0.7, 1.4, 2.8, 5.6, 11.25, 22.5, 45, 90% saliva) and incubated for 30 min at room temperature before the mix was diluted 10-fold onto Vero E6 cells (MOI 0.3). For cell treatment Vero E6 cells were incubated with saliva for 30 min at 37°C and then inoculated with ZIKV MR766 (concentrations: 0.018, 0.035, 0.07, 0.14, 0.28, 0.56, 1.125, 2.25, 4.5, 9% saliva). 2 hours later, medium was changed and 2 days later infection rates were determined by a cell-based immunodetection assay that enzymatically quantifies the flavivirus protein E. (b) Vero E6 cells in Ibidi slides were inoculated with ZIKV MR766 (MOI 35) in the presence of saliva and incubated for 2 hours at 4°C. The inoculum was removed and immunofluorescent staining directed against flavivirus protein E was performed. Cell nuclei were stained with Hoechst 33342. Attached virus particles were imaged by confocal microscopy (see Fig. S1) and quantified using ImageJ (Fiji). (c) Vero E6 cells were inoculated with pooled saliva and infected with different dilutions of ZIKV MR766 resulting in MOI 36.5, 9.1, 2.3, 0.57 and 0.14. Thereafter, it was proceeded as in a). The relative infection for saliva titration (left) and for 10% saliva (right) is shown. Data in a) and c) are normalized to infection rates in the absence of the respective sample and represented as average values obtained from triplicate infections ± standard deviations.
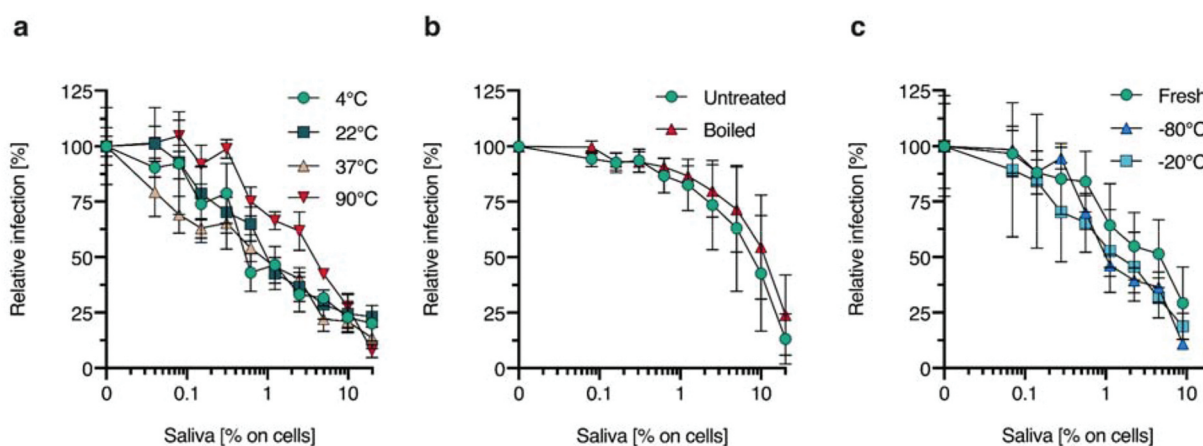
Figure 4. Stability of the anti-ZIKV factor in saliva. (a) Pooled saliva which was incubated at 4°C, 22°C, 37°C or 90°C for 1 hour was serially diluted, mixed 2:1 with ZIKV MR766 and incubated for 30 min at room temperature. The mix was added onto Vero E6 cells (MOI 0.3) resulting in indicated concentrations. 2 hours later, medium was changed and 2 days later infection rates were determined by a cell-based immunodetection assay that enzymatically quantifies the flavivirus protein E. (b) Saliva from five individual donors was boiled at 99°C for 20 min and centrifuged for 15 min with 20,000 × g. Supernatants and untreated saliva samples were serially diluted and added onto Vero E6 cells, which were subsequently infected with ZIKV MR766 (MOI 0.15). Then, it was proceeded as in a). The figure shows the average of the quantified infection rates from the five donors. (c) Pooled saliva which was fresh or has been frozen at −20°C or −80°C for 3 hours was serially diluted, mixed 10:1 with ZIKV MR766 and incubated for 30 min at room temperature. The mix was added onto Vero E6 cells (MOI 0.3) and it was proceeded as in a). Data in a)-c) are normalized to infection rates in the absence of the respective sample and represented as average values obtained from triplicate infections ± standard deviations.

semen EVs were heat-resistant, inhibited ZIKV attachment to target cells and were broadly active against different ZIKV strains [38]. Thus, we prepared salivary EVs (saEVs) by applying a filtration-ultrafiltration (F-UF) protocol. Nanoparticle tracking analysis (NTA) of the resulting saEV preparation (concentrated approx. 23-fold by volume from the original saliva pool) revealed 7.4×10^{10} particles per ml with a mean size distribution of 175.2 nm (108.6 nm span, 145.8 nm peak size) (Figure 5(a) right). For comparison, in the saliva pool used for EV preparation, we detected 3.86×10^{10} particles per ml with a mean size distribution of 218.3 nm (125.4 nm span, 190.5 nm peak size) (Figure 5(a) left). Western blot analysis of saliva and the saEV preparation showed the presence of the EV-specific markers tetraspanin CD9 and lipid-raft-associated flotillin-1 (Figure 5(b)) in both the pooled saliva samples and the EV preparation. Abundant salivary proteins α-amylase and lysozyme were also detected, with lysozyme being slightly depleted and α-amylase slightly concentrated in the EV preparation (Figure 5(b)). Transmission electron microscopy finally confirmed the presence of vesicle-like structures in saliva and the saEV preparation (Figure 5(c)).

We next titrated particle-normalized amounts of saEVs and saliva on cells and infected with ZIKV. As shown in Figure 6(a), the F-UF prepared saEVs suppressed ZIKV infection in a dose-dependent manner

with an IC_{50} of 1.9×10^9 particles per ml. A similar IC_{50} (2.3×10^9 particles per ml) was obtained for saliva. Time-of-addition experiments then demonstrated that saEVs block ZIKV only if present during viral entry (SaEV + ZIKV), but not if vesicles were added 2 hours post-infection (ZIKV → SaEV) or incubated for 2 hours on cells but removed prior to infection (SaEV → ZIKV) (Figure 6(b)). Confocal microscopy imaging of attached virions showed that increasing concentration of saEVs indeed prevents ZIKV attachment to cells (as shown above for whole saliva (Figure 3(b) and S1)), suggesting that saEVs occupy cellular structures important for viral attachment (Figure 6(c) and S2). In agreement with the data obtained with saliva (Figure 4(b)), boiling did not considerably alter the antiviral activity of saEVs (Figure 6(d)), suggesting that denaturable proteins are not responsible for the anti-ZIKV activity of saliva. Next, we subjected saEVs to proteinase K digestion which resulted in almost complete degradation of all proteins (Figure 6(e)). Again, the resulting saEV sample retained its anti-ZIKV activity (Figure 6 (d)), further indicating that neither soluble proteins nor peptides but EVs in saliva are responsible for blocking ZIKV. Lastly, we prepared EV-depleted saliva by ultrafiltration of undiluted saliva. NTA of the flow-through (containing material <100 kDa) revealed a reduction in particles numbers by 2.0 and 2.2 orders of magnitude compared to PBS-reconstituted retentate
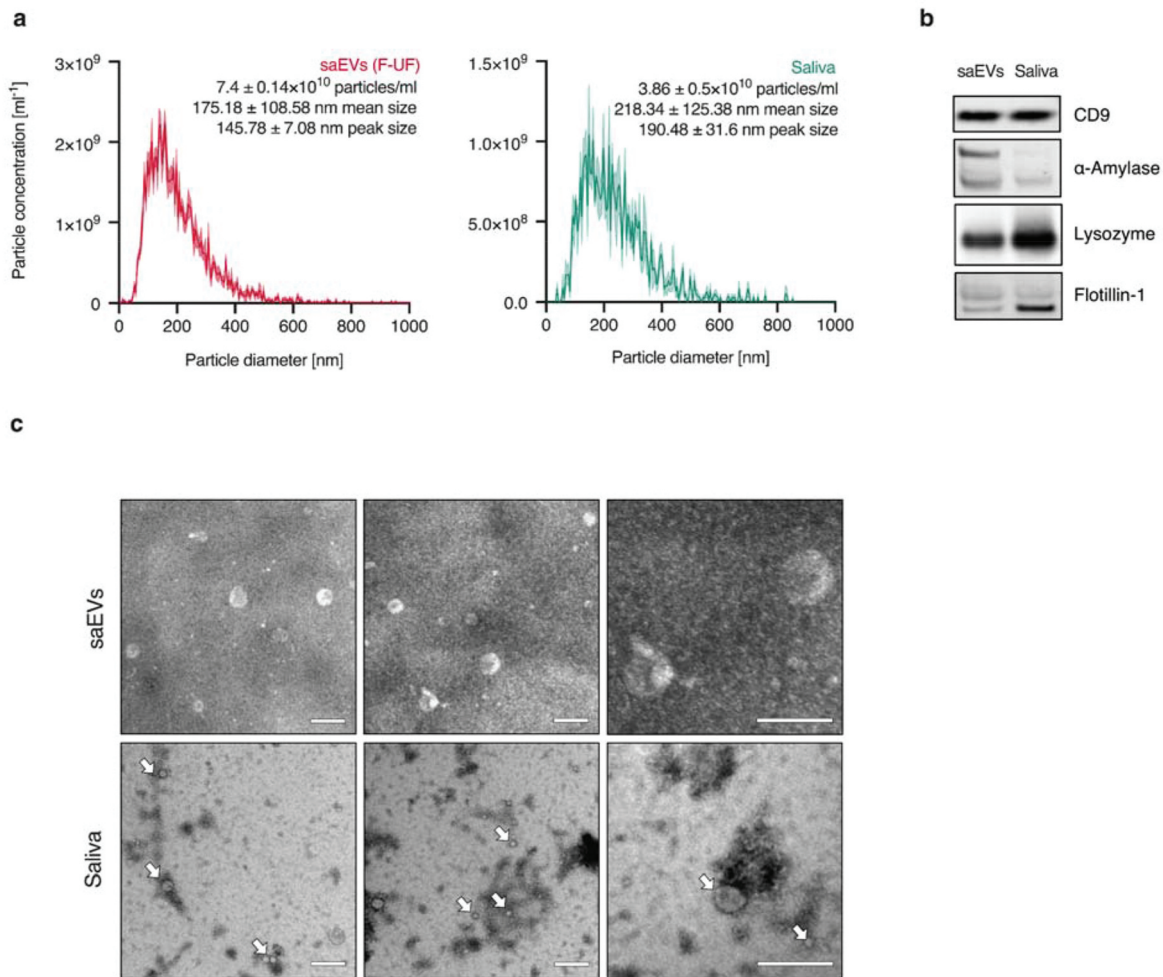
Figure 5. Isolation and characterization of salivary EVs (saEVs). (a) F-UF enriched saEVs (left) and the corresponding saliva pool used for EV preparation (right) were analysed by nanoparticle tracking analysis to determine the concentration and the distribution of extracellular vesicles/free-floating particles. (b) Detection of EV (CD9, flotillin-1) and salivary protein (lysozyme, α-amylase) markers in protein-concentration normalized samples of saliva and saEVs by western blot. (c) Saliva and saEVs were adsorbed on glow discharged carbon-coated copper grids for 1 min at room temperature and negatively stained with 2% (w/v) uranyl acetate in H_2O. Dried samples were imaged with a transmission electron microscope. Scale bar: 200 nm.

or untreated saliva, respectively. Accordingly, a substantial loss in antiviral activity was detected (Figure 6(f)) further confirming that the majority of the anti-ZIKV activity can be attributed to saEVs.

SaEVs purified by tangential flow filtration/bind-elute size exclusion chromatography inhibit ZIKV infection

SaEVs prepared by the above applied F-UF protocol still contain non-vesicular proteins and impurities such as lysozyme (Figure 5(b)) which may introduce a bias in the downstream experiments and could potentially contribute to the observed antiviral effects. Therefore, we next purified and characterized saEVs consistent with the MISEV2018 guidelines [39]. To this end, we

isolated EVs from a saliva pool of 10 donors by applying 0.22 μm filtration, tangential flow filtration (TFF), followed by bind-elute size exclusion chromatography (BE-SEC). This methodology results in an EV preparation where neither extra-vesicular RNA nor soluble contaminating proteins are detected [35]. This preparation contained 1.6×10^{11} particles per ml with a mean size distribution of 183.5 nm (107.1 nm span, 160.4 nm peak size) (Figure 7(a)) which is slightly larger than in the previous preparation (Figure 5(a)) and in line with further depletion of smaller material. For reference, we also performed NTA on the unpurified saliva pool and found 2.23×10^{10} particles per ml and, as previously, a slightly larger mean particle size of 219.2 nm. This saEVs preparation was enriched in CD9, flotillin-1 as well as ALG-2-interacting protein X (Alix), which is
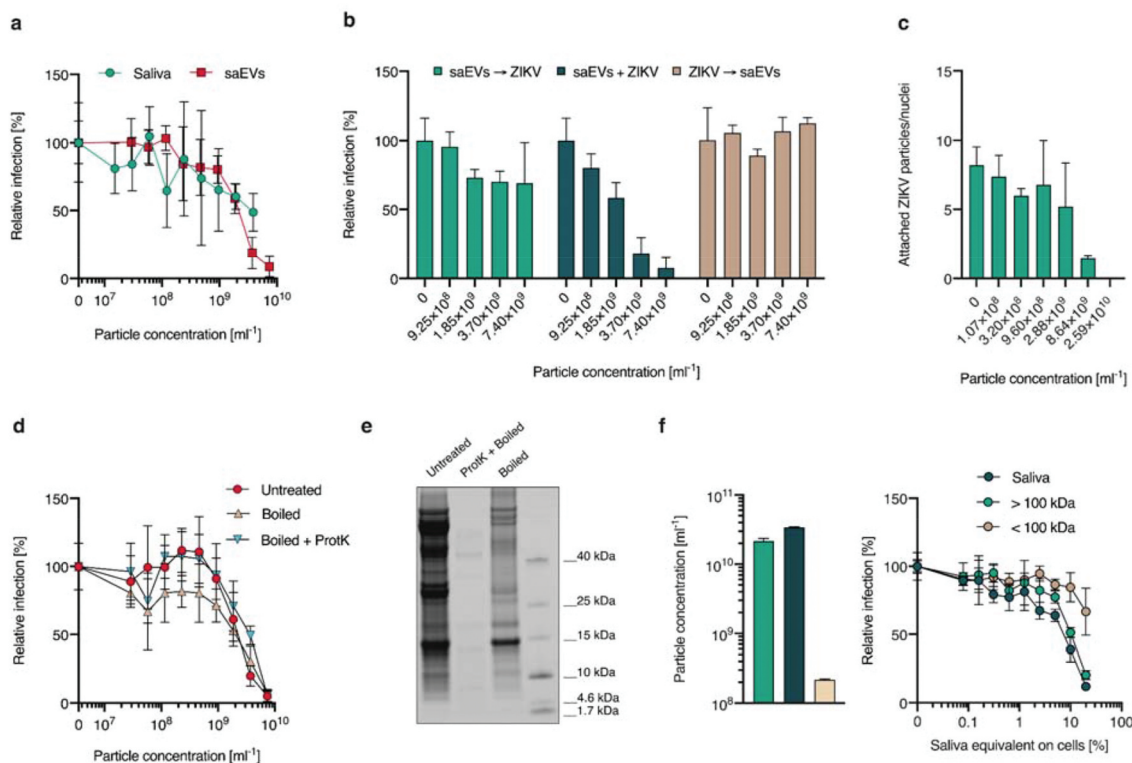
Figure 6. SaEVs inhibit ZIKV infection through inhibiting viral attachment. (a) Vero E6 cells were inoculated with serially diluted saliva or saEVs, of which the particle numbers were determined, and infected with ZIKV MR766 (MOI 0.15). 2 hours post-infection, medium was changed and 2 days later infection rates were determined by a cell-based immunodetection assay that enzymatically quantifies the flavivirus protein E. (b) Vero E6 cells were inoculated with (i) first saEVs and then, after a washing step, ZIKV 2 hours later (SaEVs→ZIVK); (ii) saEVs and ZIKV simultaneously (SaEVs+ZIKV) or first ZIKV and then, after a washing step, saEVs 2 hours later (ZIKV→SaEVs). After another 2 hours, medium was changed and 2 days later infection rates measured by the immunodetection assay. (c) Vero E6 cells in Ibidi slides were inoculated with ZIKV MR766 (MOI 35) in the presence of saEV preparations and incubated for 2 hours at 4℃. The inoculum was removed and immunofluorescent staining directed against flavivirus protein E was performed. Cell nuclei were stained with Hoechst 33342. Attached ZIKV virions were imaged by confocal microscopy (see Fig. S2) and quantified using ImageJ (Fiji). (d) SaEVs were boiled at 99℃ for 20 min and centrifuged for 15 min with 20,000 × g. One sample was additionally incubated with 300 µg/ml proteinase K for 2 hours at 37℃, following another boiling and centrifugation step. These supernatants and the untreated saEV preparation were serially diluted and added onto Vero E6 cells, which were subsequently infected with ZIKV MR766 (MOI 0.15). Then, it was proceeded as in a). (e) The saEV samples from d) were separated by SDS-PAGE and proteins were stained with GelCode Blue stain for 1 hour. Image was taken on a LI-COR near-infrared imager. f) Pooled saliva was ultrafiltrated (cut-off: 100 kDa) and the particle concentrations of flowthrough (< 100 kDa), retentate (reconstituted in PBS, > 100 kDa) as well as corresponding untreated saliva was determined performing NTA (left). These samples were added onto Vero E6 cells and cells were infected with ZIKV MR766 (MOI 0.15). Then, it was proceeded as in a) (right). Data in a), b), d) and f) are normalized to infection rates in the absence of the respective sample and represented as average values obtained from triplicate infections ± standard deviations.

associated with the endosomal sorting complex required for transport (ESCRT) (Figure 7(b)). The above described slight concentration of α-amylase and depletion of lysozyme (Figure 5(b)) was considerably more pronounced in this preparation (Figure 7(b)), further confirming the successful purification of EVs from soluble proteins. To further characterize the surface protein composition of the isolated saEVs, we performed a bead-based multiplex EV assay. This optimized assay facilitates the detection of 37 different candidate EV surface markers previously described [36,37]. We regularly detected expression of EV markers CD9, CD63, and CD81, as well as CD14, CD24,

CD44, CD133, CD142, and CD326 when using a mix of (Figure 7(c)) or individual (Fig. S3) anti-CD9, -CD63, -CD81 tetraspanin detection antibodies. We then tested this highly purified saEV preparation for its effect on ZIKV infection. Similar to the previous results, TFF/BE-SEC purified saEVs potently and dose-dependently inhibited ZIKV infection with an IC$_{50}$ of 4.76×10^9 particles per ml (Figure 7(d)). Further corroborating our previous findings, boiling and proteinase K treatment of the sample did not result in loss of the antiviral activity (Figure 7(d)) even though the most protein was degraded (Figure 7(e)). In line with this, the morphology of the saEVs remained unchanged
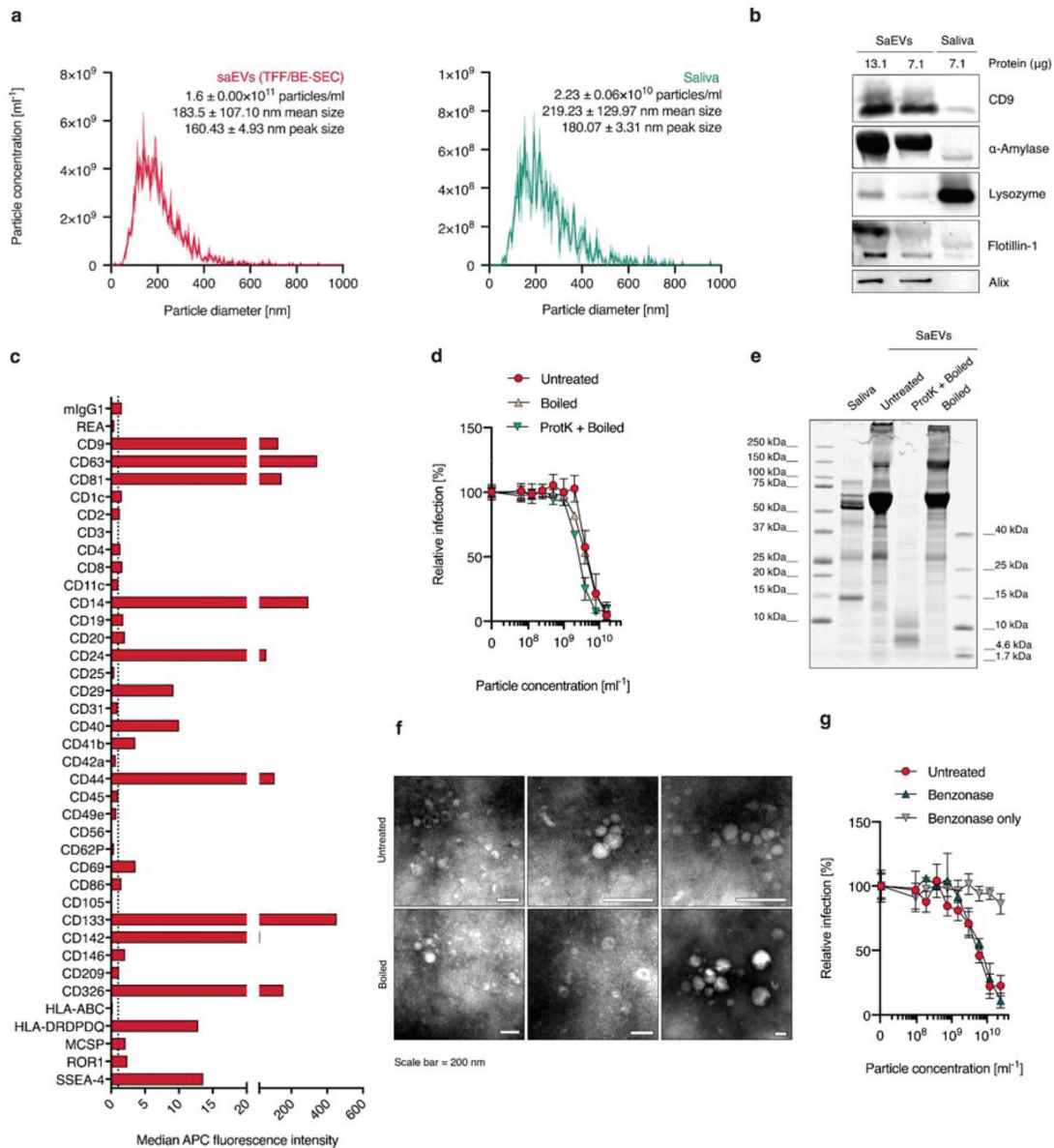
Figure 7. TFF/BE-SEC purified saEVs inhibit ZIKV. (a) TFF/BE-SEC purified saEVs (left) and the corresponding saliva pool used for EV preparation (right) were analysed by NTA to determine the concentration and the size distribution of EVs/free-floating particles. (b) Detection of EV (CD9, flotillin-1, Alix) and salivary protein (lysozyme, α-amylase) markers in saliva and saEVs by western blot. (c) Characterization of the saEV surface protein composition was performed by multiplex bead-based flow cytometry using a mixture of anti-CD9, anti-CD63, and anti-CD81 detection antibodies (see Fig. S3 for single stainings). Background-subtracted median fluorescence APC intensity values are shown for 37 candidate EV markers and two internal isotype controls (mIgG1 and hIgG1 (REA)). (d) SaEVs were left untreated, boiled at 99°C for 20 min and centrifuged for 15 min with 20,000 × g, or treated with 300 μg/ml proteinase K for 2 hours at 37°C, following another boiling and centrifugation step and used for further experiments. Samples were serially diluted and added onto Vero E6 cells, which were subsequently infected with ZIKV MR766 (MOI 0.15). 2 hours post-infection, medium was changed and 2 days later infection rates were determined by a cell-based immunodetection assay that enzymatically quantifies the flavivirus protein E. (e) Saliva and the differently treated saEVs (d) were separated by SDS-PAGE and proteins were stained with GelCode Blue stain for 1 hour. Image was taken on a LI-COR near-infrared imager. (f) Untreated and boiled saEVs were adsorbed on glow discharged carbon-coated copper grids for 1 min at room temperature and negatively stained with 2% (w/v) uranyl acetate in H$_2$O. Dried samples were imaged with a transmission electron microscope. Scale bar: 200 nm. (g) SaEVs were incubated with 25 U Benzonase® Nuclease for 2 h at room temperature with mild shaking. Samples were then serially diluted in PBS and added onto Vero E6 cells, which were subsequently infected with ZIKV MR766 as described in d). Data in d) and g) are normalized to infection rates in the absence of the respective sample and represented as average values obtained from triplicate infections ± standard deviations.
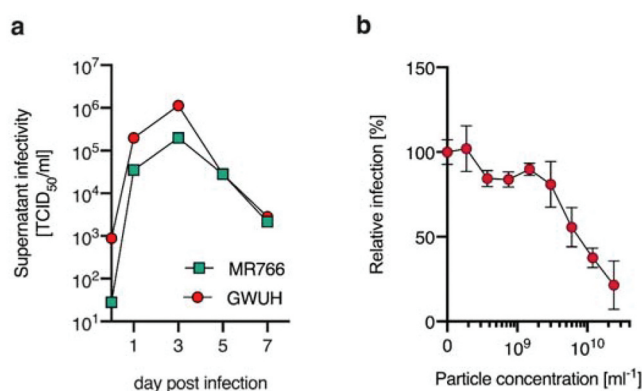
Figure 8. Primary gingival fibroblasts are productively infected by ZIKV, but infection is inhibited by saEVs. a) Primary gingival fibroblasts were infected with ZIKV MR766 or GWUH (MOI 8) and supernatant was collected on 0, 1, 3, 5 and 7 dpi. By performing $TCID_{50}$ endpoint titration $TCID_{50}$/ml was determined according to Reed and Muench. (b) Primary gingival fibroblasts were inoculated with serially diluted saEVs, of which the particle number was determined, and infected with ZIKV MR766 (MOI 5). 2 hours post-infection, medium was changed and 2 days later infection rates were determined by the cell-based immunodetection assay that enzymatically quantifies the flavivirus protein E. Data in b) are normalized to infection rates in the absence of the respective sample and represented as average values obtained from triplicate infections ± standard deviations.

after boiling (Figure 7(f)). To exclude a contribution of EV surface-associated nucleic acids on the antiviral activity, we digested purified saEVs with Benzonase nuclease, which degrades all forms of DNA and RNA. This treatment did not affect antiviral activity of saEVs (Figure 7(g)), confirming that EVs are the responsible factor in saliva that suppress ZIKV infection.

SaEVs inhibit ZIKV infection of primary oral cells

In order to confirm that ZIKV infection and its inhibition by saEVs also occur in relevant target cells, we used primary gingival fibroblasts and first infected them with ZIKV strains MR766 and GWUH. Indeed, cells released infectious progeny virions with increasing titres following infection (Figure 8(a)), showing that they are productively infected and could serve as portal of entry for the virus. Moreover, as demonstrated on different cell types previously (Figure 2), also infection of gingival fibroblasts was inhibited by purified saEVs (Figure 8(b)). This further corroborates a target-cell independent mode of action and relevance in preventing oral transmission.

The anti-ZIKV activity of saliva is donor-dependent

Results shown so far were obtained with pooled saliva or EV preparations derived thereof. To clarify whether the

anti-ZIKV activity is a general feature of human saliva, we analysed cell-free samples derived from 11 individual donors without flavivirus disease but vaccination history (Table S1). All samples dose-dependently suppressed infection, but with different potencies (Figure 9(a)). At the highest tested saliva concentration of 10%, eight specimens inhibited ZIKV by more than 50%, and three (#9, #10 and #11) of them by even more than 95%. The mean IC_{50} for all eleven samples was 3.28 ± 1.7% of saliva (Figure 9(a), Table A1, see Appendix). However, cell viability assays performed in the absence of virus (but otherwise identical conditions) showed that four saliva samples (#3, #9, #10 and #11) caused a dose-dependent reduction in the metabolic activity of the cells below 75% (Figure 9(b)). Thus, anti-ZIKV activities calculated for these samples have to be interpreted with caution. The adjusted mean IC_{50} for the remaining non-cytotoxic samples was 4.43 ± 0.74% (Table A1). The observed variation in potencies between donors could not be explained by vaccination status (Table S1) but raised the question, whether these effects are donor- or donation-dependent. We therefore analysed samples collected from two donors over the course of a day for inhibition of ZIKV infection and found IC_{50}s ranging from 0.70% to 3.00% (2.0 ± 1.0%) for donor 6, and 0.68% – 1.05% (0.9 ± 0.2%) for donor 8 (Figure 9(c)), and reduced metabolic activities to up to 68% (Figure 9(d)). This indicates that the anti-ZIKV activity may be conserved within an individual and does not substantially vary between donations. In conclusion, all analysed saliva samples suppressed ZIKV infection, the antiviral activity varied between individual donors, but interpretation of the antiviral activity is sometimes confounded by salivary compounds affecting cell metabolism.

Potent inhibition of ZIKV infection by saEVs derived from individual donors

We next enriched saEVs from the same 11 saliva samples that were analysed above using the F-UF protocol. NTA analyses of the unprocessed saliva samples revealed an average concentration of 3.05×10^{10} (min: 1.2×10^{10}; max: 6.33×10^{10}) particles per ml saliva with a mean particle diameter of 208.7 nm (min: 181.1 nm; max: 227.6 nm) (Fig. S4, Table A1). The saEV preparations had an average concentration of 1.08×10^{11} particles per ml, and an average diameter of 184 nm (min: 160.6 nm; max: 203.8 nm) (Fig. S4, Table A1). EV preparations derived from saliva samples that reduced cell viability maintained this activity (see #3, #9, #10 and #11) (Figure 10(a)) showing that the F-UF protocol to enrich EVs did not allow to remove the responsible toxic factors. There was no correlation between the diameter of particles in saliva and saEV

Figure 9. Anti-ZIKV activity of saliva is donor-dependent. (a) Vero E6 cells were inoculated with serially diluted saliva from 11 donors and infected with ZIKV MR766 (MOI 0.3). 2 hours post-infection, medium was changed and 2 days later infection rates were determined by a cell-based immunodetection assay that enzymatically quantifies the flavivirus protein E. Data are normalized to infection rates in the absence of the respective sample and represented as average values obtained from triplicate infections ± standard deviations. (b) Vero E6 cells were incubated with the saliva samples from a) at indicated concentrations for 2 hours. Medium was then replaced and the cellular viability determined 2 days later by MTT assay. Data are normalized to metabolic activity in the absence of saliva. (c) Vero E6 were inoculated with serially diluted saliva from donors 6 and 8 (as in Figure 9(a-b) taken at different times of day and infected with ZIKV MR766 (MOI 0.15). 2 hours post-infection, medium was changed and 2 days later infection rates were determined as described in a). (d) The samples from c) were assessed for effects on cellular metabolic activity by MTT assay.

(Figure 10(b) left), suggesting that during sample processing other detectable non-EV particles were lost. Next, we determined the anti-ZIKV activity and effects on cellular metabolic activity of the saEV preparations as described above for saliva (see Figure 9). Every saEV preparation analysed inhibited ZIKV infection, in most cases by more than 95% (Figure 10(a)). The mean IC$_{50}$ was 1.73×10^9 particles per ml (Table A1). The highest antiviral activity

was observed for EVs from donor #10 (IC$_{50}$ of 2.5×10^8 particles per ml), and lowest for donor #5 (IC$_{50}$ of 3.8×10^9 particles per ml) (Figure 10(a)). Comparing the IC$_{50}$ values of the saEVs (Fig. S5, Table A1) with the corresponding activities and particle concentrations of saliva revealed a strong correlation (Figure 10(b) middle), demonstrating that EVs in this body fluid are responsible for ZIKV inhibition. Thus, saliva and saEVs inhibit ZIKV infection in
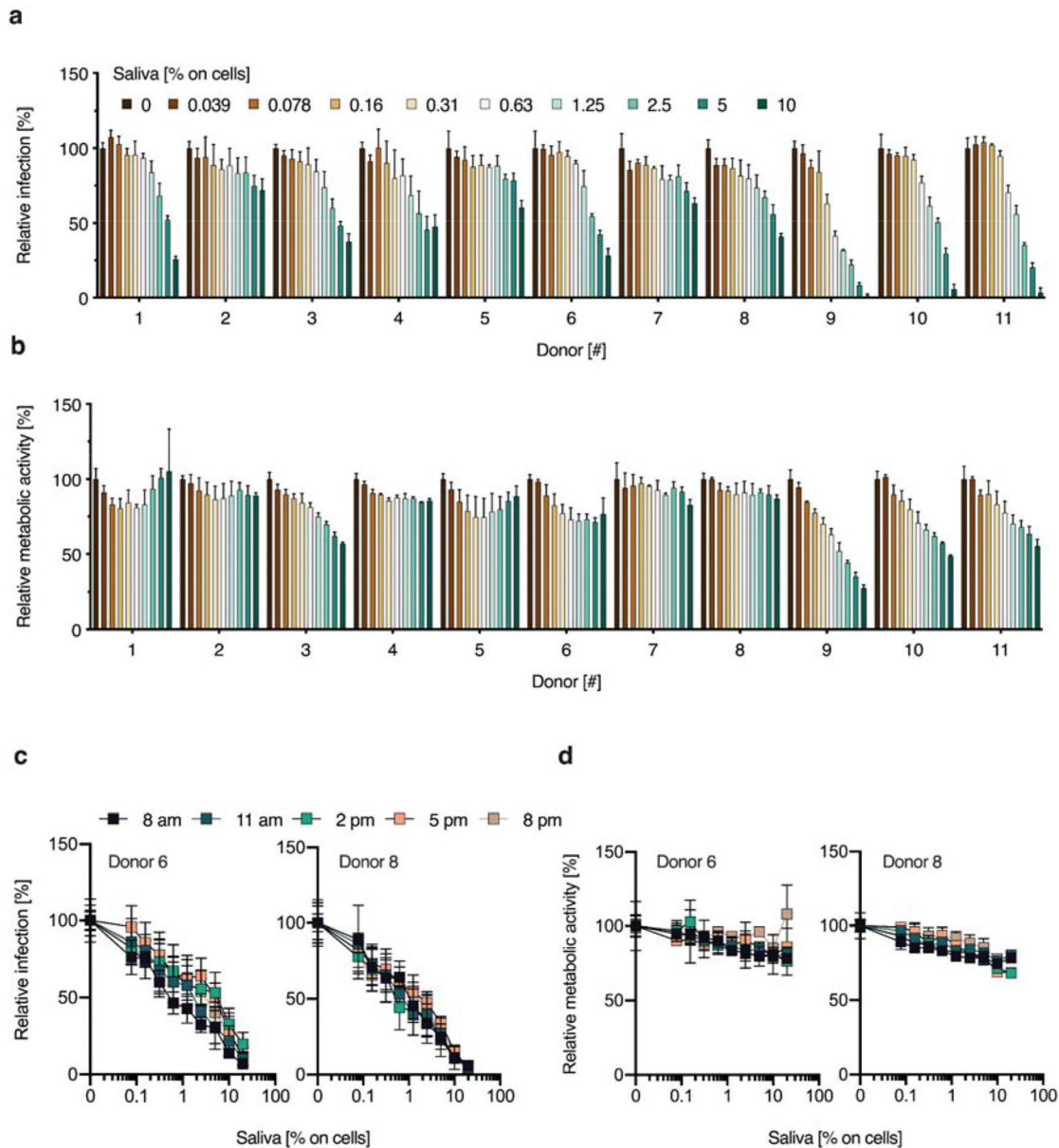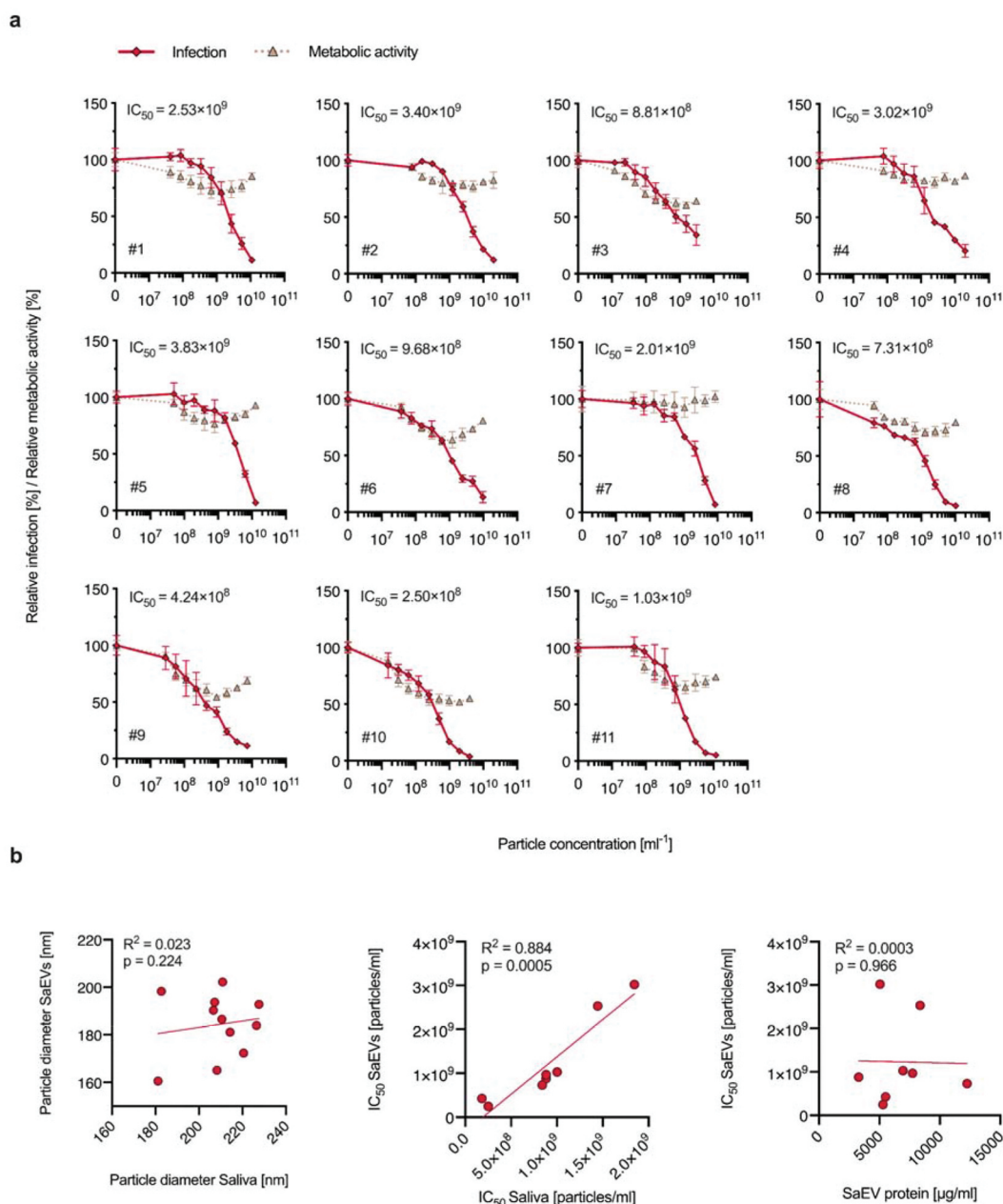
Figure 10. Anti-ZIKV activity of saEVs is donor-dependent. (a) Vero E6 cells were inoculated with serially diluted saEV preparations from 11 individual donors (see Figure 8 and S4) and treated with medium to determine effects on viability or infected with ZIKV MR766 (MOI 0.3). 2 hours post-inoculation, medium was changed and 2 days later cell viability or infection rates were determined by MTT-based or a cell-based immunodetection assay, respectively. Inhibition curves were used to calculate IC_{50}. Infection data are normalized to infection rates in the absence of the respective sample and represented as average values obtained from triplicate infections ± standard deviations. Viability data are normalized to metabolic activity in the absence of saliva. (b) Correlational analysis of the saEV and saliva particle diameter (left), or the saEV and saliva IC_{50}s (in particles per ml, see Fig. S5) (middle) or the saEV protein concentration (right). Pearson correlation coefficients, two-tailed p-value.

a dose-dependent manner with variable efficacy. We did not observe a correlation between the anti-ZIKV activity and the protein content of individual saEV samples (Figure 10(b) right), confirming results presented above (Figures 4 (b and d) that salivary proteins or peptides do not contribute to virus inhibition.

EVs from urine, vaginal lavage, and urine inhibit ZIKV but are less potent than saEVs

We previously found EVs from semen to inhibit ZIKV in a similar fashion to the here described saEVs [38]. To test, whether anti-ZIKV EVs are a more general antiviral feature of body fluids, we analysed the
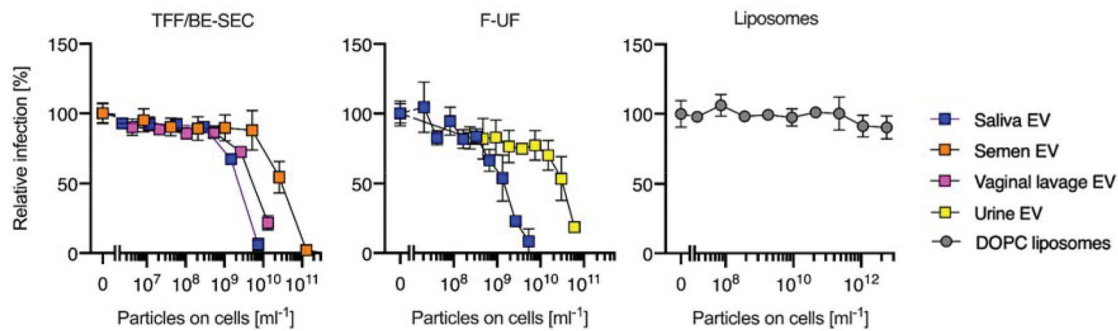
Figure 11. EVs from urine, vaginal lavage, and urine inhibit ZIKV but are less potent than saEVs. EVs were purified from saliva, semen and vaginal lavage by TFF/BE-SEC (left) or enriched from saliva and urine by F-UF (middle). These EV preparations, of which the particle number was determined, as well as DOPC liposomes (right), were used to inoculate Vero E6 cells, which were subsequently infected with ZIKV MR766 (MOI 0.15). 2 hours post-infection, medium was changed and 2 days later infection rates were determined by the cell-based immunodetection assay that enzymatically quantifies the flavivirus protein E. Data are normalized to infection rates in the absence of the respective sample and represented as average values obtained from triplicate infections ± standard deviations.

antiviral activities of EVs purified and concentrated by TFF/BE-SEC from saliva, semen, and vaginal lavage, or enriched by F-UF from saliva and urine. Interestingly, all isolated vesicles inhibited ZIKV, however with substantial differences in potencies. While saEVs proofed most potent with IC$_{50}$s of 1.1×10^9 (F-UF enrichment) or 2.1×10^9 (TFF/BE-SEC purification) particles per ml, vaginal lavage, urine, and semen showed IC$_{50}$s of 4.9×10^9, 2.6×10^{10}, or 2.7×10^{10} particles per ml, respectively (Figure 11). To exclude a general effect of high concentrations of particles unspecifically interfering with viral attachment, we included 1,2-dioleoyl-sn-glycero-3-phosphocholine (DOPC) liposomes as a control. Unlike biological EVs, these synthetic particles did not affect ZIKV infection, arguing for specific interactions being necessary to exert the anti-ZIKV effect.

Saliva and saEVs do not inhibit SARS-CoV-2 infection

We here show that EVs in saliva prevent infection by ZIKV – a virus that has not been reported to be transmitted via this body fluid. In contrast, the severe acute respiratory coronavirus 2 (SARS-CoV-2) is primarily spread via droplets from the oral cavity. This virus caused a pandemic following its emergence at the end of 2019 [40] and is readily detected in the saliva of infected individuals [41]. We thus compared the effect of saliva from 10 donors on ZIKV and SARS-CoV-2 infection. Cytotoxic effects on both target cells were only marginal (Fig. S1) and we confirmed a potent and donor-dependent inhibition of ZIKV infection (Figure 12(a)). In contrast, no antiviral effect was observed for SARS-CoV-2 isolates from the Netherlands or France

(Figure 12(b and c)). In line with this, TFF/BE-SEC purified saEVs did not inhibit SARS-2-CoV-2 infection (Figure 12(d)). Thus, saliva and saEVs do not unspecifically inhibit virus infection, but rather exert a specific effect on certain viruses which matches their dominant route of transmission.

Discussion

The main finding of our study is that human saliva has anti-ZIKV activity at physiological concentrations. The maximum ZIKV RNA levels detected in saliva were 5.9×10^4 [26], 7.4×10^4 [28], or 3×10^6 [24] RNA copies per ml, respectively. In our assays, we applied virus doses within this range (MOI 0.15–0.3 corresponds to 5.2×10^4–1.03×10^5 RNA copies per ml) and observed a potent inhibition of ZIKV infection in the presence of only 10% of saliva. Virus inhibition was observed with fresh and frozen pooled saliva (Figure 4(c)) as well as saliva from individual donors (Figures 9 and 12). Moreover, saliva consistently inhibited infection of African and Asian/American ZIKV strains in simian and human cells (Figure 2), suggesting a broad anti-ZIKV activity. The antiviral activity is temperature-stable (Figure 4) and directed towards the target cell (Figure 3(a)) since saliva reduced viral attachment rates (Figure 3(b)). The anti-ZIKV activity of saliva is conserved (average IC$_{50}$ 3.28%), but varies between donors with IC$_{50}$ values as low as 0.55% but sometimes also exceeding 10% of saliva (Figure 9(a), Table A1). Donor variations were expected, as saliva composition and flow rates are highly variable and impacted by, e.g. diet [42], hydration and physical activity [43]. However, while we did observe substantial variations between individual

Figure 12. Saliva and saEVs inhibit ZIKV but not SARS-CoV-2 infection. (a) Serially diluted saliva from 10 donors was mixed 1:1 with ZIKV MR766 and incubated for 30 min at 37℃. Then, mixture was used to inoculate Vero E6 cells (MOI 0.15). 3 hours post-infection, medium was changed and 2 days later infection rates were determined by a cell-based immunodetection assay that enzymatically quantifies the flavivirus protein E. (b and c) Serially diluted saliva from 10 donors was mixed 1:1 with SARS-CoV-2 isolates from the Netherlands or France and incubated for 30 min at 37℃. Then mixture was used to inoculated Caco-2 cells (MOI 0.003 or 0.009). 3 hours post-infection, medium was changed and 2 days later infection rates were determined by a cell-based immunodetection assay that enzymatically quantifies the spike protein S. (d) Serially diluted saEVs, which have been purified by TFF/BE-SEC, were added onto Caco-2 cells and subsequently infected with a French SARS-CoV-2 isolate (MOI 0.005). Medium was changed 2 hours later, and infection was quantified 2 days post-infection performing the immunodetection assay that quantifies the spike protein S. Data are normalized to infection rates in the absence of the respective sample and represented as average values obtained from triplicate infections ± standard deviations.

donors, repeated sampling of two donors throughout the course of a day revealed only moderate variability for one donor and remarkable consistency for another one (Figure 9). This variation is unlikely explained by flavivirus exposure of the donor (Table S1) but suggests that there might be inherent differences between individuals regarding the secretion of (antiviral) EVs in saliva, of which the basis remains to be discovered. We note that in some cases, individual saliva samples exerted effects on the metabolic activity of target cells which may interfere with the interpretation of the inhibition data (Figure 9(b)). However, saliva concentrations required to inhibit ZIKV were substantially lower than those affecting the cell, and most saliva samples did not reduce cell viability but were antivirally active.

Human saliva is mostly composed of water (99%) and several minor components including mucus, digestive enzymes, growth factors, cytokines, immunoglobulins, antibacterial peptides, bacterial cells, salts and low molecular weight metabolites [44,45]. Several components in saliva have been described to have antiviral activity, such as lysozyme, salivary lactoperoxidase, defensins, salivary agglutinin, secretory leukocyte protease inhibitor and lactoferrin [30]. However, only bovine lactoferrin has been successfully tested for specific anti-ZIKV activity before, but with conflicting results [46,47]. To identify the factor(s) responsible for ZIKV inhibition, we exposed saliva to boiling which results in protein denaturation. Interestingly, we found that this treatment did not abrogate antiviral efficacy (Figure 4(b)), suggesting that neither of the

above-mentioned factors or other enzymes or polypeptides significantly contribute to saliva's anti-ZIKV activity. This thermo-resistance and the described prevention of viral attachment by targeting the cell are reminiscent to the properties of antiviral EVs that we recently isolated from seminal plasma and that are responsible for the potent anti-ZIKV activity of human semen [38]. We thus enriched and purified EVs from pooled saliva samples by filtration-ultrafiltration (F-UF) (Figure 5) or tangential flow filtration bind-elute size exclusion chromatography (TFF/BE-SEC) (Figure 7), respectively, and showed that they, similar to saliva, dose-dependently inhibit ZIKV infection of Vero E6 cells (Figure 7(d, g)) as well as primary oral fibroblasts (Figure 8). We found that they reduced ZIKV attachment to target cells (Figure 6(c)) and are resistant to boiling (Figure 6 (d)), proteinase (Figure 7(d)) and nuclease digestion (Figure 7(g)). In contrast, depletion of particles from saliva by ultrafiltration decreased its antiviral activity (Figure 6(f)). This confirms that neither proteins, peptides, DNA nor RNA but the EVs are the salivary factor responsible for ZIKV inhibition.

SaEV preparation by F-UF allowed the enrichment of EVs, but achieved only minor purification as evidenced by minor depletion of saliva marker lysozyme and similar levels of EV marker CD9 (Figure 5(b)). In contrast, TFF/BE-SEC purification yielded an EV isolation with substantial lysozyme depletion and CD9 enrichment (Figure 7(b)), indicating a much greater degree of purification. This also allowed detection of Alix (Figure 7(b)), which has been described to be contained in saEVs [48–50] but was undetectable in saliva (Figure 7(b)) or F-UF enriched EVs (not shown). In both saEV isolations α-amylase appeared to be enriched. The enzyme is abundant in saliva [51] and while its inclusion into EVs to a minor extent has been discussed [52], it is more likely that α-amylase interacting with EVs was co-purified. We can, however, exclude any confounding antiviral effect of this enzyme, as the band likely corresponding to α-amylase in SDS-PAGE (above 50 kDa) completely disappeared after proteinase K treatment, yet antiviral activity was unaltered (Figure 7(d, e)).

The saEV preparations by F-UF or TFF/BE-SEC derived from pooled saliva contained 7.4×10^{10} or 1.6×10^{11} particles per ml, respectively, with an average size distribution of 175.2 ± 108.6 nm or 183.5 ± 107.1 nm, and a peak at 145.8 nm or 160.4 nm (Figures 5(a), 7(a)). This suggests that the biophysical properties of saEVs were similar after applying the different isolation techniques and thus independent of EV purity. Slight size differences

might be attributed to non-EV particles that are detected by NTA in the less pure F-UF sample but removed following BE-SEC. Notably, particle-normalized amounts of pooled saliva and isolated saEVs inhibited ZIKV infection with similar efficacy. Almost complete viral inhibition was achieved with either preparation method, yielding IC_{90} values of 8×10^9 and 1.2×10^{10} particles per ml for F-UF and TFF/BE-SEC preparation of EVs, respectively, which is well below the average concentration of particles we measured in saliva (3.05×10^{10} particles per ml). Thus, both the F-UF enriched and the highly purified TFF/BE-SEC saEVs efficiently inhibit ZIKV infection showing that they are a major factor responsible for the observed anti-ZIKV activity of saliva.

NTA of individual saliva samples revealed an average concentration of 3.05×10^{10} particles per ml with an average size distribution of 208.8 nm (Table A1). These size and concentration ranges are in line with published studies where saEVs were isolated using conventional ultracentrifugation protocols [53–55]. This particle concentration is approximately 100–1,000 times lower than that of EVs in semen ($\sim 10^{12-13}$ particles per ml [56,57]). However, saEVs show a 10-fold higher potency than semen EVs when analysed side-by-side (Figure 11). Neglecting the ratio of actual EVs to non-EV particles, their numbers and composition in different body fluids might differ drastically.

These differences may partially explain why saliva (mean IC_{50} 3.28%) is less effective in blocking ZIKV infection than semen (mean IC_{50} of 0.74% [38]). In line with this, EVs derived from vaginal lavage and urine, but not plain lipid vesicles, also showed anti-ZIKV effects (Figure 11). This suggests that body fluids generally contain EVs that have a certain feature that renders them active against ZIKV. The number of EVs and their different intrinsic anti-ZIKV activities, however, might determine the activity of the respective body fluid.

EVs are a heterogeneous mixture of membranous particles released from cells via the endosomal pathway or by budding from the plasma membrane, and are involved in multiple physiological and pathological processes [58]. Saliva harbours plenty of EVs, that contain and transfer RNA and proteins and are assumed to play a role in the oral microenvironment or wound healing, but whose ultimate function is unclear [50,58]. We found that salivary EVs competitively block ZIKV attachment to target cells. Saliva contains on average 3.05×10^{10} EVs per ml, which exceeds the maximum concentration of Zika virions detected in this body fluid by four to five orders of

magnitude [24,26,28] and is well sufficient to block ZIKV infection. The exact mechanism by which saEVs (and those derived from semen [38], vaginal lavage and urine (Figure 11)) inhibit ZIKV attachment and the identification of the EV species and composition responsible for anti-ZIKV activity and its cellular target is subject of ongoing research.

To test whether saliva and saEVs generally inhibit virus infection, we worked with the recently emerged SARS-CoV-2 that is also shed into saliva and can be transmitted via respiratory droplets. The absence of any effect of saliva or saEVs on SARS-CoV-2 infection (Figure 12) suggests that SARS-CoV-2 transmission via saliva is not prevented by the body fluid and suggests that saEVs do not unspecifically interfere with virus infection but to have a more specific mechanism. It is intriguing, however, to speculate that saEVs may also block other flaviviruses such as Dengue or West Nile Virus, as previously shown for seminal EVs [38].

In conclusion, our results show that EVs in human saliva prevent ZIKV but not SARS-CoV-2 infection which may help to explain why ZIKV is typically not transmitted via deep kissing – despite the fact that saliva contains high levels of ZIKV RNA [10,11,23–27] and infectious virus [24,28] during infection, and the susceptibility of oral cells to ZIKV infection (Figure 8). Ultimately, EV-mediated inhibition of virion attachment represents a novel and very elegant innate defence mechanism against invading viruses – offering prospects for novel prophylactic or therapeutic interventions.

Disclosure statement

A.G. and S.E.A. are consultants for and have equity interest in Evox Therapeutics, Oxford, UK. All other authors declare no conflict of interest.

ORCID

Rüdiger Groß http://orcid.org/0000-0003-0355-7915
André Görgens http://orcid.org/0000-0001-9198-0857
Samir El Andaloussi http://orcid.org/0000-0003-4468-9113
Jan Münch http://orcid.org/0000-0001-7316-7141

References

[1] Grubaugh ND, Ladner JT, Kraemer MUG, et al. Genomic epidemiology reveals multiple introductions of Zika virus into the USA. Nature. 2017;546 (7658):401–405. .

[2] Duffy MR, Chen T-H, Hancock WT, et al. Zika virus outbreak on yap island, federated states of micronesia. N Engl J Med. 2009;360(24):2536–2543.

[3] Cao-Lormeau V-M, Blake A, Mons S, et al. Guillain-Barré Syndrome outbreak associated with Zika virus infection in French Polynesia: a case-control study. Lancet. 2016;387(10027):1531–1539.

[4] Krauer F, Riesen M, Reveiz L, et al. Zika virus infection as a cause of congenital brain abnormalities and guillain–barré syndrome: systematic review. PLOS Med. 2017;14(1):e1002203.

[5] Rasmussen SA, Jamieson DJ, Honein MA, et al. Zika virus and birth defects — reviewing the evidence for causality. N Engl J Med. 2016;374(20):1981–1987.

[6] Nielsen-Saines K, Brasil P, Kerin T, et al. Delayed childhood neurodevelopment and neurosensory alterations in the second year of life in a prospective cohort of ZIKV-exposed children. Nat Med. 2019;25(8):1213–1217.

[7] World Health Organization. Zika epidemiology update [Online]. 2019. Available from: https://www.who.int/emergencies/diseases/zika/epidemiology-update/en/

[8] Musso D, Ko AI, Baud D. Zika Virus Infection — after the Pandemic. N Engl J Med. 2019;381(15):1444–1457.

[9] European Centre for Disease Prevention and Control. Zika virus disease in Var department, France [Online]; 2019. Available from: https://www.ecdc.europa.eu/sites/default/files/documents/RRA-Zika-France-16-Oct-2019-corrected.pdf

[10] Grischott F, Puhan M, Hatz C, et al. Non-vector-borne transmission of Zika virus: A systematic review. Travel Med Infect Dis. 2016;14(4):313–330.

[11] Paz-Bailey G, Rosenberg ES, Doyle K, et al. Persistence of Zika virus in body fluids — final report. N Engl J Med. 2018;379(13):1234–1243.

[12] Musso D, Nhan T, Robin E, et al. Potential for Zika virus transmission through blood transfusion demonstrated during an outbreak in French Polynesia, November 2013 to February 2014. Eurosurveillance. 2014;19(14):20761.

[13] Driggers RW, Ho C-Y, Korhonen EM, et al. Zika virus infection with prolonged maternal viremia and fetal brain abnormalities. N Engl J Med. 2016;374(22):2142–2151.

[14] Musso D, Roche C, Robin E, et al. Potential sexual transmission of Zika Virus. Emerg Infect Dis. 2015;21(2):359–361.

[15] Moreira J, Peixoto TM, Siqueira AM, et al. Sexually acquired Zika virus: a systematic review. Clin Microbiol Infect. 2017;23(5):296–305.

[16] Counotte MJ, Kim CR, Wang J, et al. Sexual transmission of Zika virus and other flaviviruses: A living systematic review. PLOS Med. 2018;15(7):e1002611.

[17] Colt S, Garcia-Casal MN, Peña-Rosas JP, et al. Transmission of Zika virus through breast milk and other breastfeeding-related bodily-fluids: A systematic review. PLoS Negl Trop Dis. 2017;11(4):e0005528.

[18] Centers for Disease Control and Prevention (CDC). Clinical guidance for healthcare providers for prevention of sexual transmission of Zika virus [Online]. 2019. Available from: https://www.cdc.gov/zika/hc-providers/clinical-guidance/sexualtransmission.html

[19] Siqueira WL, Moffa EB, Mussi MCM, et al. Zika virus infection spread through saliva–a truth or myth? Braz Oral Res. 2016;30(1):19–21.

[20] Leão J, Gueiros L, Lodi G, et al. Zika virus: oral healthcare implications. Oral Dis. 2017;23(1):12–17.

[21] Swaminathan S, Schlaberg R, Lewis J, et al. Fatal Zika virus infection with secondary nonsexual transmission. N Engl J Med. 2016;375(19):1907–1909.

[22] Foy BD, Kobylinski KC, Foy JLC, et al. Probable non–vector-borne Transmission of Zika Virus, Colorado, USA. Emerg Infect Dis. 2011;17(5):880–882.

[23] Musso D, Roche C, Nhan T-X, et al. Detection of Zika virus in saliva. J Clin Virol. 2015;68:53–55.

[24] Barzon L, Pacenti M, Berto A, et al. Isolation of infectious Zika virus from saliva and prolonged viral RNA shedding in a traveller returning from the Dominican Republic to Italy, January 2016. Eurosurveillance. 2016;21(10):30159.

[25] Nicastri E, Castilletti C, Liuzzi G, et al. Persistent detection of Zika virus RNA in semen for six months after symptom onset in a traveller returning from Haiti to Italy, February 2016. Eurosurveillance. 2016;21(32):30314.

[26] Barzon L, Pacenti M, Franchin E, et al. Infection dynamics in a traveller with persistent shedding of Zika virus RNA in semen for six months after returning from Haiti to Italy, January 2016. Eurosurveillance. 2016;21(32):30316.

[27] Bingham AM, Cone M, Mock V, et al. Comparison of test results for Zika Virus RNA in urine, serum, and saliva specimens from persons with travel-associated Zika Virus Disease — florida, 2016. MMWR Morb Mortal Wkly Rep. 2016;65(18):475–478.

[28] Bonaldo MC, Ribeiro IP, Lima NS, et al. Isolation of infective Zika virus from urine and saliva of patients in Brazil. PLoS Negl Trop Dis. 2016;10(6):e0004816.

[29] Newman CM, Dudley DM, Aliota MT, et al. Oropharyngeal mucosal transmission of Zika virus in rhesus macaques. Nat Commun. 2017;8(1):169.

[30] Malamud D, Abrams WR, Barber CA, et al. Antiviral activities in human saliva. Adv Dent Res. 2011;23(1):34–37.

[31] Dick GW, Kitchen S, Haddow A. Zika Virus (I). Isolations and serological specificity. Trans R Soc Trop Med Hyg. 1952;46(5):509–520.

[32] Lanciotti RS, Lambert AJ, Holodniy M, et al. Phylogeny of Zika Virus in Western Hemisphere, 2015. Emerg Infect Dis. 2016;22(5):933–935.

[33] Shatzkes K, Teferedegne B, Murata H. A simple, inexpensive method for preparing cell lysates suitable for downstream reverse transcription quantitative PCR. Sci Rep. 2015;4(1):4659. 2014.

[34] Aubry M, Richard V, Green J, et al. Inactivation of Zika virus in plasma with amotosalen and ultraviolet A illumination. Transfusion. 2016;56(1):33–40.

[35] Corso G, Mäger I, Lee Y, et al. Reproducible and scalable purification of extracellular vesicles using combined bind-elute and size exclusion chromatography. Sci Rep. 2017;7(1):11561.

[36] Dryden KA, Wieland SF, Whitten-Bauer C, et al. Native hepatitis B virions and capsids visualized by electron cryomicroscopy. Mol Cell. 2006;22(6):843–850.

[37] Wiklander OPB, Bostancioglu RB, Welsh JA, et al. Systematic methodological evaluation of a multiplex bead-based flow cytometry assay for detection of extracellular vesicle surface signatures. Front Immunol. 2018;9(JUN):1326.

[38] Müller JA, Harms M, Krüger F, et al. Semen inhibits Zika virus infection of cells and tissues from the anogenital region. Nat Commun. 2018;9(1):2207.

[39] Théry C, Witwer KW, Aikawa E, et al. Minimal information for studies of extracellular vesicles 2018 (MISEV2018): a position statement of the international society for extracellular vesicles and update of the MISEV2014 guidelines. J Extracell Vesicles. 2018;7(1):1535750.

[40] Zhu N, Zhang D, Wang W, et al. A novel coronavirus from patients with pneumonia in China, 2019. N Engl J Med. 2020;382(8):727–733.

[41] Wyllie AL, Fournier J, Casanovas-Massana A, et al. Saliva is more sensitive for SARS-CoV-2 detection in COVID-19 patients than nasopharyngeal swabs. medRxiv. 2020;04:16.20067835.

[42] Morzel M, Truntzer C, Neyraud E, et al. Associations between food consumption patterns and saliva composition: specificities of eating difficulties children. Physiol Behav. 2017;173:116–123.

[43] Tanabe M, Takahashi T, Shimoyama K, et al. Effects of rehydration and food consumption on salivary flow, pH and buffering capacity in young adult volunteers during ergometer exercise. J Int Soc Sports Nutr. 2013;10(1):49.

[44] Humphrey SP, Williamson, RT. A review of saliva: normal composition, flow, and function. J. Prosthet. Dent. 2001;85(2):162–169.

[45] Soini HA, Klouckova I, Wiesler D, et al. Analysis of volatile organic compounds in human saliva by a static sorptive extraction method and gas chromatography-mass spectrometry. J Chem Ecol. 2010;36(9):1035–1042.

[46] Carvalho CAM, Casseb SMM, Gonçalves RB, et al. Bovine lactoferrin activity against Chikungunya and Zika viruses. J Gen Virol. 2017;98(7):1749–1754.

[47] Chen J-M, Fan Y-C, Lin J-W, et al. Bovine lactoferrin inhibits dengue virus infectivity by interacting with heparan sulfate, low-density lipoprotein receptor, and DC-SIGN. Int J Mol Sci. 2017;18:1957.

[48] Gonzalez-Begne M, Lu B, Han X, et al. Proteomic analysis of human parotid gland exosomes by multidimensional protein identification technology (MudPIT). J Proteome Res. 2009;8(3):1304–1314.

[49] Yu J, Lin Y, Xiong X, et al. Detection of Exosomal PD-L1 RNA in saliva of patients with periodontitis. Front Genet. 2019;10. DOI:10.3389/fgene.2019.00202

[50] Palanisamy V, Sharma S, Deshpande A, et al. Nanostructural and transcriptomic analyses of human saliva derived exosomes. PLoS One. 2010;5 (1):e8577.

[51] Vitorino R, Lobo MJC, Ferrer-Correira AJ, et al. Identification of human whole saliva protein components using proteomics. Proteomics. 2004;4(4):1109–1115.

[52] Ogawa Y, Kanai-Azuma M, Akimoto Y, et al. Exosome-like vesicles with dipeptidyl peptidase IV in human saliva. Biol Pharm Bull. 2008;31(6):1059–1062.

[53] Winck FV, Carolina Prado Ribeiro A, Ramos Domingues R, et al. Insights into immune responses in oral cancer through proteomic analysis of saliva and salivary extracellular vesicles. Nat Publ Gr. 2015;5:16305.

[54] Sun Y, Xia Z, Shang Z, et al. Facile preparation of salivary extracellular vesicles for cancer proteomics. Sci Rep. 2016;6(1):24669.

[55] Aqrawi LA, Galtung HK, Vestad B, et al. Identification of potential saliva and tear biomarkers in primary Sjögren's syndrome, utilising the extraction of extracellular vesicles and proteomics analysis. Arthritis Res Ther. 2017;19(1):1–15.

[56] Vojtech L, Woo S, Hughes S, et al. Exosomes in human semen carry a distinctive repertoire of small non-coding RNAs with potential regulatory functions. Nucleic Acids Res. 2014;42(11):7290–7304.

[57] Ronquist G, Brody I. The prostasome: its secretion and function in man. Biochim Biophys Acta. 1985;822 (2):203–218.

[58] Yáñez-Mó M, Siljander PR-M, Andreu Z, et al. Biological properties of extracellular vesicles and their physiological functions. J Extracell Vesicles. 2015;4(1):27066.

Appendix

Table A1. Properties and antiviral activities of individual saliva samples and EVs derived thereof.

Sample Donor #	Saliva					SaEVs			
	IC_{50} [% saliva]	IC_{50} [particles/ml]	Particles [ml^{-1}] ± SD	Mean particle size [nm] ± span	Particle peak size ± SD	IC_{50} [particles/ml]	Particles [ml^{-1}] ± SD	Mean particle size (± span)	Particle peak size ± SD
1	5.10	1.45×10^{9}	$2.83 \pm 0.06 \times 10^{10}$	214.3 ± 118.9	183.5 ± 15.2	2.53×10^{9}	$11.00 \pm 0.00 \times 10^{10}$	181.1 ± 100.9	157.8 ± 9.5
2	> 10.00	$> 4.63 \times 10^{9}$	$4.63 \pm 0.06 \times 10^{10}$	208.3 ± 125.4	175.9 ± 3.1	3.40×10^{9}	$20.00 \pm 0.00 \times 10^{10}$	165.1 ± 90.0	147.0 ± 1.7
3*	4.27	8.83×10^{8}	$2.07 \pm 0.06 \times 10^{10}$	206.7 ± 139.2	164.6 ± 5.8	8.81×10^{8}	$3.10 \pm 0.10 \times 10^{10}$	190.2 ± 116.3	151.8 ± 6.7
4	4.00	1.84×10^{9}	$4.63 \pm 0.06 \times 10^{10}$	181.1 ± 100.5	156.5 ± 2.6	3.02×10^{9}	$20.00 \pm 0.00 \times 10^{10}$	160.6 ± 86.2	145.4 ± 3.9
5	> 10.00	$> 2.50 \times 10^{9}$	$2.50 \pm 0.00 \times 10^{10}$	226.5 ± 131.0	192.3 ± 12.2	3.83×10^{9}	$12.67 \pm 0.58 \times 10^{10}$	183.8 ± 111.3	155.7 ± 4.6
6	3.63	8.83×10^{8}	$2.43 \pm 0.06 \times 10^{10}$	210.9 ± 123.9	178.6 ± 3.8	9.68×10^{8}	$9.67 \pm 0.58 \times 10^{10}$	202.1 ± 101.5	171.3 ± 16.1
7	> 10.00	$> 1.93 \times 10^{9}$	$1.93 \pm 0.06 \times 10^{10}$	207.2 ± 130.3	180.6 ± 6.9	2.01×10^{9}	$8.50 \pm 0.44 \times 10^{10}$	193.7 ± 101.7	175.3 ± 4.8
8	5.03	8.39×10^{8}	$1.67 \pm 0.06 \times 10^{10}$	210.5 ± 117.3	179.6 ± 21.7	7.31×10^{8}	$10.33 \pm 0.58 \times 10^{10}$	186.4 ± 103.3	158.9 ± 4.1
9*	0.55	1.81×10^{8}	$3.27 \pm 0.06 \times 10^{10}$	227.6 ± 140.2	196.4 ± 16.8	4.24×10^{8}	$7.23 \pm 0.12 \times 10^{10}$	192.7 ± 103.8	168.0 ± 2.9
10*	2.09	2.50×10^{8}	$1.20 \pm 0.1 \times 10^{10}$	182.7 ± 117.9	152.8 ± 7.5	2.50×10^{8}	$3.97 \pm 0.25 \times 10^{10}$	198.2 ± 115.1	172.9 ± 9.9
11*	1.58	1.00×10^{9}	$6.33 \pm 0.15 \times 10^{10}$	220.5 ± 131.9	184.4 ± 25.3	1.03×10^{9}	$11.67 \pm 0.58 \times 10^{10}$	172.3 ± 109.7	146.3 ± 1.1
Average	3.28	9.16×10^{8}	$3.05 \pm 0.15 \times 10^{10}$	208.8 ± 125.1	176.8 ± 11.0	1.73×10^{9}	$10.74 \pm 0.29 \times 10^{10}$	184.2 ± 100.9	159.1 ± 6.8
Average (w/o *)	4.43	1.25×10^{9}	$2.95 \pm 0.05 \times 10^{10}$	208.4 ± 121.1	178.1 ± 9.3	2.35×10^{9}	$13.17 \pm 0.31 \times 10^{10}$	181.8 ± 90.0	158.8 ± 6.4

IC_{50} (inhibition of ZIKV MR766 MOI 0.15 infection) are given in % (see Figure 9a) and in particles/ml for saliva (see Fig. S5) and for saEV isolations (see Figure 10a). All NTA data (see Fig. S4) is given as the mean of three measurements, in the case of particle concentration and peak size ± standard deviation (SD). Mean particle size is reported ± mean span of the size distribution. For mean peak size, the major (> 50%) peak of the size distribution is reported in case of multiple peaks. Average values are given for all donors and excluding donors with pronounced cytotoxicity in inhibition experiments (defined as reaching < 75% relative metabolic activity at the highest dose of saliva/saEV used). Donors where 50% inhibition was not reached for saliva samples (#2, #5, #7) were excluded from average IC_{50} calculations. *, reduced cell viability